

The 1.88 Ga Kotalahti and Vammala nickel belts, Finland: geochemistry of the mafic and ultramafic metavolcanic rocks



STEPHEN J. BARNES^{1,*}, HANNU V. MAKKONEN^{2,3)}, SARAH E. DOWLING^{1,4)},
ROBIN E.T. HILL^{1,4)}, PETRI PELTONEN^{5,6)}

¹⁾*CSIRO Exploration and Mining, P.O. Box 1130, Bentley, W.A. 6102, Australia*

²⁾*Geological Survey of Finland, P.O. Box 1237, FI-70211 Kuopio, Finland*

³⁾*Present address: Leimaajantie 7, FI-70150 Kuopio, Finland*

⁴⁾*Present address: Triodia Exploration, Lacey St., Beckenham, Australia*

⁵⁾*Geological Survey of Finland, P.O. Box 96, FI-02151 Espoo, Finland*

⁶⁾*Present address: Northland Exploration Finland Oy, Ahventie 4, FI-02170 Espoo, Finland*

Abstract

The mafic and ultramafic volcanic rocks within the Svecfennian (1.88 Ga) Kotalahti and Vammala Nickel Belts, Finland, are spatially associated and coeval with a suite of mineralized mafic–ultramafic intrusions. They have been divided into five suites based on major element geochemistry and spatial distribution: the Rantasalmi high- and low-Mg suites, the Vammala high-Mg suite, and the Rantasalmi, Kestilä and Pielavesi low-Mg suites. The Rantasalmi and Vammala high-Mg suites are very similar and probably comagmatic, and the Kestilä and Rantasalmi low-Mg suites are derived from them by a combination of fractionation and crustal assimilation. The Pielavesi suite is interpreted as an unrelated suite of island-arc affinity. On the basis of their trace element contents, the Kotalahti Belt intrusions are comagmatic with part of the analyzed volcanic rocks. In the Vammala Belt it is likely that the parent magmas to the intrusions and picrite magmas have a common mantle source but have evolved along distinct paths, and the picrites probably do not represent parent magmas tapped directly from the intrusions. Platinum-group element data show localised evidence for depletion by sulfide extraction. Vammala picrites are predominantly S-undersaturated, with the exception of lavas in the Stormi area. In the Kotalahti Belt the volcanic rocks are predominantly S-undersaturated, while the volcanic rocks in the more northern part of the Belt are predominantly S-saturated. These spatial differences imply that the PGE contents of the metavolcanic rocks can be used as regional area selection criteria for intrusive nickel-copper-(PGE) deposits within the Finnish Svecfennian.

Keywords: platinum, nickel, sulfides, ultramafics, volcanic rocks, picrite, Svecfennian, Finland

* Corresponding author e-mail: steve.barnes@csiro.au

I. Introduction

Platinum group element depletion in volcanic suites has been identified as a signature of sulfide liquid saturation and magmatic ore formation in associated

intrusions following pioneering studies of the Siberian Traps sequence at Noril'sk (Brügmann et al., 1993) and elsewhere (Barnes & Picard, 1993; Barnes et al.,

1993). Similar signatures have since been found in the continental flood basalts of Greenland (Philipp et al., 2001) and the Emeishan province of China (Song et al., 2006). Testing the model requires the recognition of mineralized intrusions with juxtaposed comagmatic volcanic rocks. The Svecfennian terrain of Finland potentially offers such an opportunity.

The purpose of this study was to investigate the geochemical relationships between the metavolcanic rocks and coeval intrusions of the 1.88 Ga Kotalahti and Vammala Nickel Belts, which form part of the Svecfennian orogenic belt in the central part of the Fennoscandian Shield. A particular goal was to determine whether volcanic rocks could be shown to be comagmatic with mineralized intrusions, and if so, whether this relationship is reflected in depleted platinum-group element signatures in the lavas.

The geochemistry of the intrusions in the belt, and contrast between mineralized and barren intrusions, has been the subject of papers by Mäkinen (1987), Peltonen (1995a), Makkonen (1996), Mäkinen & Makkonen (2004), Lamberg (2005), Makkonen et al. (2008).

1.1 Geological setting: the Svecfennian Domain in Finland

The Svecfennian Domain of the Fennoscandian Shield covers the central and southern parts of Finland and much of Sweden, and adjoins the Archaean Domain which extends from Russia into central Finland (Fig. 1). It forms part of a series of provinces or belts of broadly similar age containing nickel sulfide mineralisation and occurring along the margins of Archaean cratons, including the Pechenga and Räglaan (Cape Smith) belts (Barnes et al., 2001; St. Onge et al., 1997).

The largest Svecfennian plutonic complex in Finland is the Central Finland Granitoid Complex (CFGC, c. 1.88 Ga), which is separated from the Archaean basement in the NE by the Palaeoproterozoic schist belt hosting several volcanogenic massive sulfide deposits (e.g. Pyhäsalmi, Vihanti) and magmatic nickel sulphide deposits (e.g. Kotalahti, Hitu-

ra). A narrow part of the belt has been named the Kotalahti Nickel Belt by Gaál (1972). In this study however, the name Kotalahti Nickel Belt applies to a larger area, which is also known in Finland as the Raahe–Ladoga Belt. Another nickel-bearing belt, the Vammala Nickel Belt, runs in NW–SE direction southwest of the CFGC (Fig. 1).

The predominant supracrustal rocks of the Svecfennian Domain are variably migmatized turbidites. Svecfennian volcanic rocks form major belts, but also occur in narrow discontinuous belts or limited occurrences within both metasedimentary and intrusive complexes. The Svecfennian volcanic rocks occurring in Finland belong to c. 1.92 and 1.88 Ga age groups (Kousa & Lundqvist, 2000, and references therein). The younger Svecfennian volcanic rocks, which are exactly of the same age as the nickeliferous ultramafic intrusions of the Thompson belt in Canada (Hulbert et al., 2005) are studied in this work.

The Svecfennian orogeny in Finland produced a series of 1.88 Ga mafic-ultramafic intrusions around the CFGC in which, according to Nironen (1997) and Peltonen (2005), the mafic magma intruded in tensional structures above a subduction zone. Many of these intrusions contain nickel sulfide mineralization. These Svecfennian nickel sulfide deposits have played a major role in Finnish nickel mining history. Altogether nine deposits have been mined beginning in 1941 at Makola (Puustinen et al., 1995) and mining still at Hitura, which has become the largest nickel mine in Finland (15 Mt @ 0.6 % Ni and 0.2 % Cu). The total production of the Svecfennian nickel mines in Finland is at present about 43 Mt @ 0.7 % Ni. The total pre-mining resource of all the deposits known to date is about 60 Mt @ 0.7 % Ni.

Intrusions are synkinematic, and emplacement took place during the maximum intensity of deformation and metamorphism (Mäkinen & Makkonen, 2004; Makkonen, 2005; Peltonen, 2005). The country rocks surrounding the intrusions were in most cases extensively metamorphosed and deformed during the early stage of the Svecfennian orogeny (Gaál, 1980; Kilpeläinen, 1998; Koistinen, 1981; Mäki-

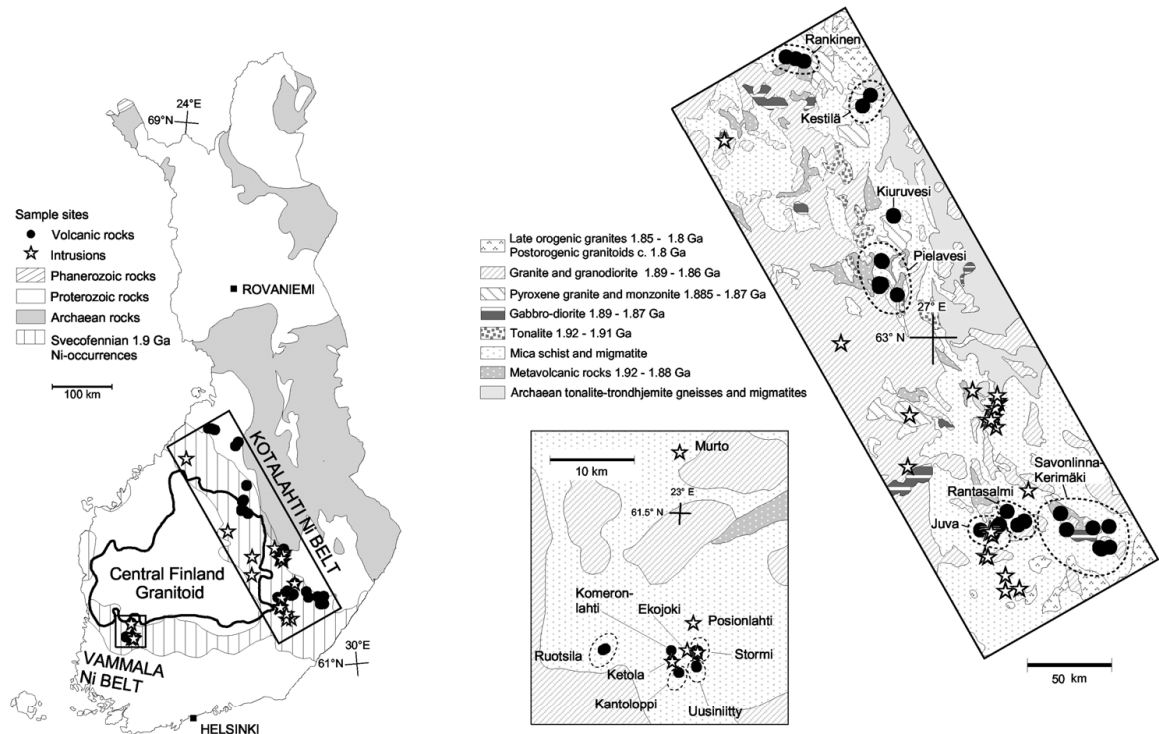


Fig. 1. Location map showing relationship of the Kotalahti and Vammala Nickel Belts to geology of the Finnish portion of the Fennoscandian Shield, and location of samples. Lithology simplified after Korsman et al. (1997).

nen & Makkonen, 2004). Overthrusting and faulting resulted in fragmentation of both the intrusions and the country rocks. Different tectonic conditions produced intrusions with pronounced variations in size, shape and lithology (cf. Papunen & Gorbunov, 1985). Owing to the synorogenic timing of the magmatism the intrusions have a very complicated tectonomagmatic history. This makes the Svecofennian intrusions quite different when compared to anorogenic nickel sulfide bearing intrusions like Sudbury, Voisey's Bay and Noril'sk (Mäkinen & Makkonen, 2004), but similar deposits are known in the Sveconorwegian and Grenville Belts (Boyd & Mathieson, 1979; Boyd et al., 1988).

The Svecofennian nickel-bearing mafic and ultramafic intrusions are mainly found within migmatitic mica gneisses, although in the Kotalahti Nickel Belt some occur within or at the contact of the Archaean gneisses. The intrusions often form oval shaped bod-

ies of varying dimensions in surface plan, the largest ones up to 10 km in length, and include gabbroic, peridotitic or composite gabbro-peridotite types.

Two main types of intrusion have been identified by Mäkinen (1987), named Vammala Type and Kotalahti Type after the belts in which they predominate, and characterised by the abundance of clinopyroxene and orthopyroxene, respectively. Makkonen (1996) interpreted the mineralogical differences as being due to differences in the degree of country rock contamination. Peltonen (2005) concluded that the Kotalahti Belt intrusions, which were emplaced through the sialic Archaean crust or the Primitive Arc Complex, were more likely to become contaminated by SiO_2 and crystallize orthopyroxene. In the Vammala Belt the main contaminant was carbonaceous and calcareous sulfidic black schist material resulting in early sulfide and clinopyroxene saturation in the melt.

Peltonen (1995a) conducted a comparative study of barren and mineralized intrusions from the Vammala Nickel Belt in order to constrain ore-forming processes in more detail. The main conclusion was that all intrusions have been contaminated by sulfide-rich metasediments (black schists) resulting in the formation of an immiscible sulfide phase in all intrusions. The critical variable is the timing of this sulfide saturation. Olivines show uniformly low Ni abundances indicative of extensive and early sulfide segregation. In the Kotalahti Belt, the barren intrusions never reached sulfide saturation, while barren intrusions in Vammala reached sulfide saturation and segregated sulfides prior to the emplacement of the magma to the present erosion level. The mineralized intrusions in the Vammala Nickel Belt crystallized from magmas that had segregated only small amounts of sulfides as implied by their depletion in platinum-group elements but not in nickel. Sulfide segregation was an *in-situ* process in the dynamic feeder dike environment represented by the mineralized Vammala Nickel Belt intrusions.

Makkonen et al. (2008) classified the Kotalahti Belt intrusions into three groups: 1) mineralized, 2) intermediate and 3) barren on the basis of the amount and composition of the sulfides found in each intrusion. The whole-rock geochemical results show evidence of country rock contamination in mineralized intrusions. Contamination is best seen in elevated $\text{Al}_2\text{O}_3/\text{CaO}$ ratio and Zr, P_2O_5 , Th and LREE contents in peridotites. Olivines in mineralized intrusions show nickel depletion, which in some intrusions is seen to have taken place *in situ*. Barren intrusions contain nickel-undepleted olivines or olivines with low Fo and low Ni.

1.2. Emplacement of the Svecfennian (1.88 Ga) mafic-ultramafic intrusions

Tholeiitic magma formed both extrusions and intrusions at 1.88 Ga in the Kotalahti Nickel Belt (Makkonen, 1996) and in the Vammala Nickel Belt (Kilpeläinen, 1998). Intrusions in both areas were emplaced at different crustal levels during the mag-

ma ascent (Peltonen, 1995a, Makkonen, 1996) (cf. Fig. 2).

The following constraints can be put on the magmatic history: (a) intrusion took place near the maximum intensity of D_2 and peak of the metamorphism (Kilpeläinen, 1998; Koistinen, 1996; Mäkinen & Makkonen, 2004; Marshall et al., 1995; Peltonen 1995b, 2005), (b) most of the intrusions occur within a highly deformed/metamorphozed zone but some intrusions also on higher levels within lower-grade metamorphic rocks, (c) volcanic rocks occur usually within areas of lower metamorphic grade compared to the intrusions, but in some places they are in contact with an intrusion.

Makkonen (2005) proposed a model (Fig. 2) in which magma is intruding during D_2 within the Svecfennian collision zone. The basis of the model is the generation of a high temperature shear zone, containing abundant migmatites, between a large mantle magma reservoir and an imbrication zone of thrust folds probably above the subduction (after rifting in a collision zone). The shear zone developed at the depth of 15–20 km as indicated by the PT-calculations from spinel-bearing symplectites and reaction rims formed between cumulus olivine and intercumulus plagioclase during cooling of the intrusion (Tuisku & Makkonen, 1999).

The mafic magma probably reached the surface slightly before the main intrusive event. This volcanic event thus took place during the rifting stage in the collision zone. The close spatial association of the volcanic and intrusive rocks in the study area is largely a result of juxtaposition by thrust faulting within the Svecfennian Domain. In addition, during the later, D_3 phase, the earlier sub-horizontal rock units were folded in many places into sub-vertical to vertical attitudes, juxtaposing rock units from multiple crustal levels to the present erosion level (Gaál, 1980; Koistinen et al., 1996; Kilpeläinen, 1998; Mäkinen & Makkonen, 2004). This obscures the relationship between the volcanic rocks and intrusions on a local scale.

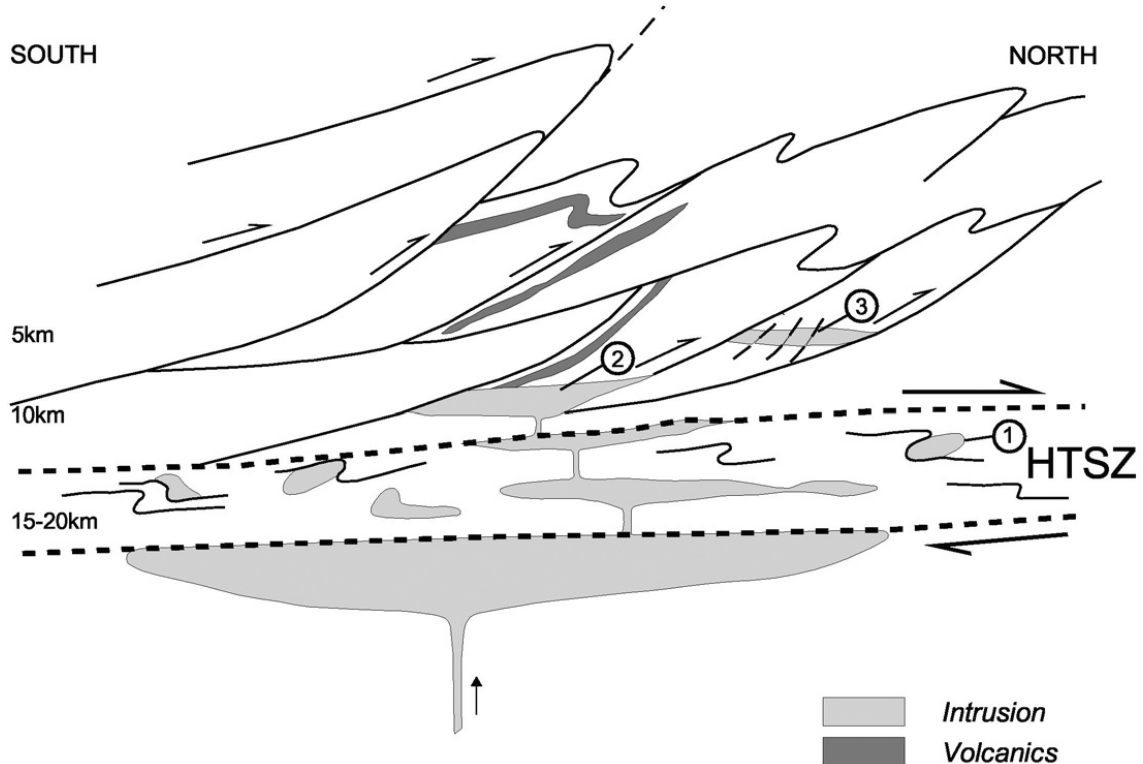


Fig. 2. Schematic vertical section of the upper crust showing the relationship of intrusions and volcanic rocks in the Kotalahti belt, simplified after Makkonen (2005). HTSZ = high temperature shear zone, marked by broken line; 1 = typical Svecofennian intrusion within the HTSZ; 2 = intrusion within lower metamorphic grade rocks, 3 = an uplifted intrusion body.

2. Analytical Methods

Whole-rock major element analyses and data for trace elements Ni, Cr, Co, V, Sr and Zn were determined on all the volcanic rocks and the Tiemasoja, Hanhisalo, Luusniemi and Rantala intrusions by X-Ray Fluorescence on fusion discs at CSIRO laboratories in Perth, Australia.

Platinum-group elements were determined by nickel sulfide fire assay on a 50 g aliquot, with Te coprecipitation and aqua regia digestion followed by ICP-MS at Geoscience Laboratories in Sudbury, Canada. Precision estimates based on duplicate analyses are listed in Table 1, and results of replicate analyses of certified standards in Table 2. Duplicate analyses agreed within 14 % or less of the average deter-

mined value for 80 % of the samples, for all the PGEs plus Au (Table 1).

Rare earth elements, Th, Y, Zr and Nb were also determined at Geoscience Laboratories by ICP-MS (method IM-101), using an open beaker dissolution by hydrofluoric, hydrochloric, perchloric and nitric acids. To test for the possible effects of non-dissolution of resistate phases, a subset of 25 samples was also analyzed using closed beaker dissolution. Zr values for the closed beaker method were higher by an average 7.9 % of the amount present, an error which is considered to be within the sampling uncertainty.

Analytical methods for the Vammala Belt intrusions and most of the Kotalahti belt intrusions are given by Peltonen (1995c) and Makkonen (1996), re-

Table 1. Estimates of analytical precision, detection limit and blanks for PGE analyses. Precision estimates based on comparison of duplicate analyses of 17 samples, expressed as median and 80th percentile of square root of squared value of error between determinations divided by average determination.

	Ir	Ru	Rh	Pt	Pd	Au	Samples
Duplicate error (median)	7.2%	10.6%	7.9%	11.4%	5.3%	9.4%	17
Duplicate error (80th percentile)	12.6%	12.9%	12.7%	13.9%	9.8%	10.1%	17
Detection limit (ppb)	0.04	0.13	0.08	0.14	0.11	0.71	
Blanks – % less than DL	100	100	100	85	85	100	12

Table 2. Results of replicate analyses (n=number of analyses) of internal standard materials by Geoscience laboratories, Sudbury, Canada, over a two year period. The values of Meisel et al. (2001) are more recent and of higher precision than the "Certified" values and are regarded as more reliable (Burnham, pers. comm., 2007)

Source	Digestion Method	Analysis Method							
			Au	Ir	Pd	Pt	Rh	Ru	
TDB-1	OGL (n=26)*	NiS-FA	ICP-Q-MS	6.21 ± 0.61	0.08 ± 0.02	22.52 ± 1.35	4.87 ± 0.35	0.45 ± 0.05	0.26 ± 0.07
	Plessen & Erzinger (1988)	NiS-FA	ICP-Q-MS	4.8 ± 1.0	0.12 ± 0.02	20.0 ± 1.7	3.8 ± 0.6	0.33 ± 0.04	0.34 ± 0.08
	Meisel et al. (2001)	HPA-S	ICP-HR-MS	N/A	0.077 ± 0.011	23.0 ± 2.9	5.02 ± 0.21	N/A	0.24 ± 0.05
	Certified			6.3 ± 1.0	0.15	22.4 ± 1.4	5.8 ± 1.1	0.7	0.3
WGB-1	OGL (n=14)	NiS-FA	ICP-Q-MS	1.84 ± 0.79	0.202 ± 0.037	12.97 ± 2.41	5.25 ± 1.56	0.198 ± 0.077	0.15 ± 0.06
	Plessen & Erzinger (1988)	NiS-FA	ICP-Q-MS	2.0 ± 0.9	0.20 ± 0.04	13 ± 1.1	3.8 ± 1.0	0.14 ± 0.01	0.20 ± 0.04
	Meisel et al. (2001)	HPA-S	ICP-HR-MS	N/A	0.27 ± 0.07	11.7 ± 1.3	4.71 ± 0.40	N/A	0.16 ± 0.02
	Certified			2.9 ± 1.1	0.33	13.9 ± 2.1	6.1 ± 1.6	0.32	0.3

*one data point for Rh rejected due to high Cu interference

Q-MS=quadrupole mass spectrometry. HR-MS = high resolution mass spectrometry (magnetic sector).

spectively. Full analytical data pertaining to this paper are given in Table 3.

3. Sample Localities

Metavolcanic rocks were sampled from localities throughout the Vammala and Kotalahti Belts (Fig. 1, Table 4). Most samples were collected using a small hand-held core-drill from cores of deformed pillows on glaciated outcrops.

3.1. Savonlinna-Kerimäki area

Sampled mafic volcanic rocks in this area occur in the zone of diopside-amphibolites of the Haukive-

si area described by Gaál & Rauhamäki (1971). According to them this zone separates the NE migmatites from the SW metaturbidites. They include in this group layered diopside-amphibolites, which is the most common type, mica-bearing skarn-amphibolites, uralite- and plagioclase porphyrites and pillow lavas. Kukonkivi represents typical mafic pillow lava. The Parkumäki, Häsvuori and Kukonkivi sampling sites belong to the 25 km long eastwest-trending volcanic zone from Parkumäki to Makkola that occurs between two large plutonic complexes, the mainly tonalitic Varparanta dome in the north and the mainly gabbroic Joutsenmäki–Tolvanniemi dome in the south. The nickel belt with the nickel bearing intrusions (e.g. Enonkoski, Hälvälä) and migmatitic mica

Table 3. Complete listing of analytical data. Major element oxides in wt.%, trace elements in ppm, PGE and Au in ppb.

Locality group	Kest LM	Kest LM	Kest LM	Kest LM	Kest LM	Kest LM	Kest LM	Kest LM
Locality	Kettukaarrot	Kettukaarrot	Kettukaarrot	Kettukaarrot	Kumpukangas	Kumpukangas	Kumpukangas	Kumpukangas
Sample	kettu-1	kettu-1	kettu-2	kettu-2	kumpu-1	kumpu-1	kumpu-2	kumpu-2
SiO ₂	50.44	50.44	49.27	49.27	47.55	47.55	48.33	48.33
TiO ₂	1.59	1.59	1.55	1.55	1.17	1.17	1.77	1.77
Al ₂ O ₃	13.84	13.84	13.43	13.43	17.66	17.66	15.97	15.97
Fe ₂ O ₃ TOT	15.14	15.14	14.95	14.95	12.38	12.38	13.16	13.16
MnO	0.23	0.23	0.23	0.23	0.18	0.18	0.23	0.23
MgO	5.85	5.85	6.62	6.62	6.08	6.08	6.03	6.03
CaO	9.74	9.74	9.71	9.71	7.45	7.45	8.61	8.61
Na ₂ O	2.63	2.63	2.53	2.53	3.55	3.55	3.04	3.04
K ₂ O	0.33	0.33	0.38	0.38	2.06	2.06	0.96	0.96
S	0.03	0.03	0.07	0.07	0.01	0.01	0.01	0.01
Cr	52	52	50	50	92	92	43	43
Ni	45	45	37	37	28	28	45	45
Cu	17	17	10	10	17	17	40	40
Zn	116	116	124	124	107	107	102	102
V	354	354	375	375	262	262	253	253
Y	27	27	28	28	22	22	24	24
Zr	92	92	95	95	73	73	98	98
Th	0.57	0.59	0.54	0.51	0.68	0.75	2.15	2.37
Nb	10.7	11.2	11	10.1	6.9	6.6	5.2	4.9
La	8.07	8.54	9.93	9.98	22.18	24.16	17.14	17.15
Ce	17.09	18.55	23.15	24.45	48.38	54.36	36.50	37.58
Pr	2.49	2.72	3.35	3.49	7.21	7.75	5.19	5.23
Nd	11.03	12.50	14.97	16.82	30.41	32.67	22.24	23.28
Sm	3.13	3.47	4.14	4.34	6.80	7.09	5.11	5.25
Eu	1.39	1.47	1.42	1.55	2.04	2.35	1.72	1.83
Gd	4.11	4.46	5.23	5.65	5.75	6.36	5.38	5.83
Dy	4.49	4.94	5.48	6.17	4.35	4.63	5.00	5.17
Tb	0.75	0.78	0.93	0.94	0.88	0.90	0.91	0.88
Ho	0.97	1.07	1.30	1.35	0.90	0.99	1.01	1.09
Er	2.69	3.03	3.47	3.87	2.41	2.67	2.70	2.86
Tm	0.44	0.46	0.50	0.56	0.36	0.38	0.40	0.43
Yb	2.71	2.73	3.21	3.35	2.23	2.27	2.79	2.53
Lu	0.43	0.46	0.54	0.53	0.33	0.36	0.42	0.42
Ir	0.29	0.29	0.29	0.29	0.00	0.00	n.a.	n.a.
Ru	0.26	0.26	0.23	0.23	0.14	0.14	n.a.	n.a.
Rh	1.20	1.20	1.09	1.09	n.a.	n.a.	n.a.	n.a.
Pt	15.60	15.60	16.10	16.10	1.89	1.89	n.a.	n.a.
Pd	16.10	16.10	13.60	13.60	1.24	1.24	n.a.	n.a.
Au	89.60	89.60	0.86	0.86	1.27	1.27	n.a.	n.a.

Kest LM	Kest LM	Kest LM	Kest LM	Kest LM	Kest LM	Kest LM				
Ritokoski	Ritokoski	Ritokoski	Ritokoski	Taku-kangas						
rito-1	rito-1	rito-2	rito-2	taku-1A	taku-1A	taku-1B	taku-1B	taku-2	taku-2	taku-3
49.55	49.55	49.22	49.22	48.15	48.15	50.13	50.13	49.78	49.78	61.12
1.57	1.57	1.61	1.61	1.66	1.66	1.52	1.52	1.98	1.98	0.66
13.94	13.94	14.39	14.39	16.02	16.02	15.98	15.98	15.40	15.40	16.08
14.51	14.51	14.81	14.81	13.31	13.31	11.84	11.84	12.87	12.87	7.01
0.22	0.22	0.23	0.23	0.20	0.20	0.18	0.18	0.19	0.19	0.11
6.01	6.01	6.59	6.59	7.02	7.02	6.88	6.88	5.58	5.58	2.57
10.31	10.31	9.74	9.74	8.63	8.63	8.25	8.25	7.90	7.90	4.44
2.53	2.53	2.99	2.99	2.66	2.66	3.15	3.15	2.91	2.91	3.08
0.24	0.24	0.16	0.16	1.18	1.18	1.02	1.02	1.87	1.87	2.54
0.03	0.03	0.02	0.02	0.12	0.12	0.07	0.07	0.10	0.10	0.54
79	79	86	86	215	215	210	210	154	154	51
69	69	71	71	59	59	56	56	31	31	16
177	177	163	163	41	41	33	33	27	27	165
96	96	98	98	121	121	96	96	122	122	87
377	377	361	361	194	194	172	172	197	197	96
29	29	27	27	30	30	19	19	31	31	20
102	102	106	106	137	137	57	57	148	148	192
0.86	0.87	0.94	0.96	1.14	1.05	2.18	2.11	1.17	1.22	8.89
6.1	6.8	5.8	6.9	5.3	5.6	4.1	4.2	9	9.5	12.6
8.08	8.08	9.27	9.07	16.22	15.98	10.14	10.10	22.57	21.78	35.58
21.88	20.01	23.21	21.92	35.89	34.44	21.69	21.11	49.45	45.97	69.12
3.32	3.05	3.46	3.35	5.11	4.89	3.00	2.93	6.99	6.48	8.54
15.84	14.53	15.98	15.23	22.99	21.29	12.75	12.35	29.56	27.40	31.57
4.30	4.15	4.66	4.38	5.51	5.29	2.99	2.98	6.41	6.32	5.96
1.53	1.42	1.51	1.45	2.08	1.91	1.33	1.16	2.22	2.10	1.43
5.44	4.87	5.51	5.04	6.34	6.00	3.22	3.18	6.87	6.33	4.99
5.54	4.96	5.54	5.01	6.03	5.57	3.08	2.91	6.30	6.06	3.88
0.87	0.86	0.94	0.88	1.01	1.01	0.53	0.49	1.08	1.02	0.72
1.14	1.05	1.18	1.10	1.28	1.18	0.63	0.65	1.31	1.30	0.77
3.22	2.78	3.19	2.93	3.43	3.28	1.87	1.63	3.63	3.42	2.05
0.46	0.42	0.45	0.43	0.52	0.50	0.27	0.26	0.56	0.53	0.29
2.71	2.84	2.75	2.71	3.04	3.07	1.61	1.58	3.14	3.26	1.81
0.42	0.41	0.39	0.42	0.49	0.47	0.25	0.25	0.52	0.50	0.32
n.a.	n.a.	n.a.	n.a.	n.a.	n.a.	n.a.	n.a.	n.a.	n.a.	n.a.
0.33	0.33	0.39	0.39	n.a.	n.a.	n.a.	n.a.	0.14	0.14	0.14
0.63	0.63	0.59	0.59	n.a.						
3.75	3.75	3.62	3.62	n.a.	n.a.	n.a.	n.a.	n.a.	n.a.	0.98
20.00	20.00	20.60	20.60	0.12	0.12	n.a.	n.a.	0.15	0.15	1.78
8.23	8.23	7.18	7.18	n.a.	n.a.	n.a.	n.a.	1.00	1.00	0.82

Kest LM	Kest LM	Kest LM	Kest LM	Kest LM	Kest LM	Piel LM	Piel LM	Piel LM
Taku-kangas	Taku-kangas	Tervahauta	Tervahauta	Tervahauta	Tervahauta	Hallaperä	Hallaperä	Hallaperä
taku-4	taku-4	terva-1	terva-1	terva-2	terva-2	Hallaperä 1	Hallaperä 2	Hallaperä 3
47.84	47.84	50.00	50.00	50.33	50.33	51.40	48.49	47.63
1.39	1.39	1.07	1.07	1.06	1.06	0.92	0.89	1.04
16.23	16.23	15.65	15.65	15.70	15.70	18.30	17.63	13.29
12.34	12.34	10.90	10.90	11.33	11.33	12.21	13.57	10.99
0.22	0.22	0.18	0.18	0.19	0.19	0.19	0.26	0.18
7.53	7.53	4.89	4.89	5.05	5.05	4.87	4.46	10.71
8.85	8.85	11.90	11.90	10.81	10.81	6.49	10.53	10.66
2.19	2.19	2.91	2.91	3.16	3.16	3.50	2.25	2.19
1.17	1.17	0.41	0.41	0.64	0.64	1.22	0.47	1.24
0.21	0.21	0.01	0.01	0.01	0.01	0.29	0.31	0.15
271	271	139	139	120	120	46	51	554
65	65	49	49	44	44	10	7	98
56	56	25	25	17	17	240	131	81
112	112	86	86	91	91	120	114	101
166	166	272	272	265	265	317	272	249
25	25	25	25	24	24	16	17	29
112	112	83	83	88	88	27	34	56
0.99	1.09	2.67	2.81	2.64	2.91	0.23	0.38	0.54
4.4	4.2	6	5.8	5.7	5.9	5.28	3.68	8.48
12.04	12.28	15.37	15.97	16.26	16.73	8.08	9.19	19.38
26.70	28.28	32.02	34.32	32.87	35.17	20.09	21.37	51.74
3.94	4.12	4.50	4.70	4.38	4.70	3.00	3.02	7.47
17.20	18.90	18.66	19.48	17.93	19.83	12.40	12.59	27.96
4.43	4.70	4.49	4.35	4.10	4.68	2.89	2.94	5.86
1.67	1.85	1.36	1.44	1.28	1.42	1.32	1.19	1.65
4.81	5.10	4.44	4.57	4.08	4.57	2.75	3.07	5.41
4.75	5.17	4.12	4.26	3.83	3.97	2.59	2.97	4.81
0.81	0.88	0.71	0.72	0.70	0.74	0.44	0.51	0.88
1.05	1.08	0.89	0.88	0.83	0.90	0.55	0.66	1.06
2.80	3.08	2.38	2.47	2.19	2.42	1.50	1.82	2.81
0.42	0.47	0.38	0.34	0.36	0.37	0.23	0.28	0.44
2.73	2.78	2.30	2.30	2.14	2.20	1.45	1.73	2.79
0.41	0.42	0.35	0.36	0.35	0.35	0.23	0.28	0.45
n.a.	n.a.	n.a.	n.a.	n.a.	n.a.	n.a.	0.03	n.a.
0.13	0.13	n.a.	n.a.	0.13	0.13	n.a.	0.14	0.12
n.a.	n.a.	0.09	0.09	n.a.	n.a.	0.09	0.13	n.a.
n.a.	n.a.	2.43	2.43	1.80	1.80	3.56	6.28	0.37
0.12	0.12	2.94	2.94	2.29	2.29	3.00	7.90	0.28
n.a.	n.a.	1.13	1.13	1.03	1.03	6.18	5.43	1.56

Piel LM	Piel LM	Piel LM	Piel LM	Piel LM	Piel LM	Piel LM				
Kärväs-järvi	Kärväs-järvi	Kärväs-järvi	Kärväs-järvi	Kärväs-järvi	Koivujoki	Koivujoki	Koivujoki	Teeri-mäki	Teeri-mäki	Teeri-mäki
Kärväs-järvi 1	Kärväs-järvi 2	Kärväs-järvi 3	Kärväs-järvi 4	Kärväs-järvi 5	Koivujoki 1	Koivujoki 2	Koivujoki 3	Teeri-mäki 1	Teeri-mäki 2	Teeri-mäki 3
49.25	50.40	51.12	49.41	52.57	56.26	54.69	49.92	49.94	50.09	51.65
1.03	0.89	1.11	1.07	0.86	0.64	0.86	0.75	0.81	1.29	0.87
14.54	15.98	17.00	15.99	18.58	18.79	17.78	19.28	11.39	15.68	15.37
12.92	11.88	11.63	10.99	9.45	7.74	8.03	10.02	15.07	11.20	12.48
0.21	0.18	0.17	0.18	0.19	0.14	0.15	0.14	0.27	0.20	0.21
4.47	5.82	3.55	4.62	2.78	2.05	3.37	5.52	8.74	6.39	5.46
13.51	10.78	9.85	13.78	8.73	7.57	8.99	8.06	10.27	8.83	9.87
2.87	2.22	3.31	2.67	4.09	2.99	3.31	3.83	1.38	3.18	2.26
0.58	0.46	0.79	0.51	0.87	1.74	1.57	1.22	0.55	1.11	0.59
0.02	0.02	0.09	0.02	0.09	0.01	0.02	0.02	0.05	0.01	0.06
86	134	65	170	41	44	34	53	181	141	125
21	36	24	38	-2	-1	1	46	42	19	20
134	66	148	109	148	48	88	15	93	10	55
115	91	97	100	112	73	90	90	103	118	79
323	329	307	298	102	100	191	146	369	253	286
15	15	16	17	28	26	27	10	17	22	17
27	41	48	35	93	85	76	26	25	10	64
0.61	0.97	0.62	0.36	0.31	2.56	1.94	1.07	0.61	0.39	0.65
4.5	5.19	4.04	3.62	8.02	6.9	6.36	3.44	3.38	3.76	5.62
7.53	8.13	7.40	6.87	15.00	10.02	9.90	8.17	5.91	23.63	16.96
16.85	17.65	17.63	15.78	34.88	22.16	23.75	17.09	14.22	50.40	37.68
2.46	2.40	2.63	2.32	5.25	3.20	3.41	2.37	2.13	7.64	5.28
10.73	9.91	11.58	10.36	22.56	14.13	15.30	10.02	9.60	32.06	20.72
2.82	2.34	3.04	2.59	5.34	3.81	4.21	2.37	2.59	6.17	4.30
1.13	0.94	1.22	1.11	1.82	1.20	1.33	0.92	0.99	2.75	1.51
3.00	2.51	3.24	2.91	5.41	4.16	4.61	2.27	2.98	5.08	3.75
2.86	2.41	3.18	2.88	4.97	4.27	4.68	1.73	2.89	3.61	3.03
0.50	0.40	0.55	0.51	0.88	0.72	0.78	0.34	0.50	0.71	0.56
0.62	0.53	0.68	0.62	1.08	0.96	1.03	0.34	0.62	0.74	0.63
1.62	1.39	1.83	1.63	2.98	2.63	2.81	0.80	1.68	1.91	1.67
0.25	0.21	0.29	0.25	0.46	0.42	0.44	0.11	0.26	0.28	0.26
1.50	1.32	1.73	1.51	2.80	2.62	2.69	0.71	1.62	1.66	1.58
0.24	0.22	0.27	0.25	0.44	0.42	0.44	0.10	0.27	0.27	0.26
0.06	0.04	n.a.	n.a.	n.a.	n.a.	n.a.	n.a.	0.03	n.a.	n.a.
0.13	0.12	0.13	0.13	0.12	0.12	0.11	0.11	0.13	0.11	n.a.
0.31	0.16	0.07	0.15	n.a.	0.03	0.04	n.a.	0.07	n.a.	0.04
12.79	2.62	2.52	3.17	0.35	1.17	1.78	0.92	1.92	0.30	1.16
27.30	3.15	4.78	3.55	0.71	0.85	2.19	0.30	1.83	0.29	1.31
6.44	2.70	4.40	7.05	6.13	1.59	2.45	1.80	2.20	0.88	2.16

| Ran HM |
|------------|------------|------------|------------|------------|------------|------------|------------|------------|------------|------------|------------|
| Mustalampi | Mustalampi | Mustalampi | Mustalampi | Pahak-kala |
| R410/18.10 | R410/24.00 | R410/30.85 | R410/31.40 | PHK1-1 | PHK2-1 | PHK3-1 | PHK3-2 | PHK4-1 | PHK5-1 | UP-1 | |
| 44.50 | 43.89 | 46.27 | 45.20 | 44.61 | 44.43 | 45.03 | 48.21 | 42.87 | 43.65 | 49.06 | |
| 0.75 | 0.70 | 1.08 | 0.99 | 0.81 | 1.30 | 1.55 | 1.36 | 0.82 | 0.96 | 1.48 | |
| 9.53 | 10.18 | 14.69 | 14.10 | 8.38 | 9.67 | 12.41 | 10.67 | 8.47 | 9.18 | 9.25 | |
| 12.43 | 13.58 | 12.05 | 12.02 | 10.25 | 12.04 | 12.22 | 11.92 | 12.58 | 12.73 | 11.74 | |
| 0.18 | 0.21 | 0.15 | 0.15 | 0.18 | 0.20 | 0.15 | 0.17 | 0.18 | 0.18 | 0.17 | |
| 21.29 | 22.30 | 10.21 | 11.48 | 14.92 | 17.90 | 13.98 | 13.31 | 19.98 | 19.30 | 13.92 | |
| 7.57 | 5.92 | 10.52 | 10.71 | 15.53 | 10.75 | 9.20 | 8.48 | 9.66 | 9.50 | 10.95 | |
| 0.25 | 0.42 | 3.20 | 2.75 | 0.59 | 0.86 | 2.15 | 2.43 | 0.28 | 0.27 | 1.72 | |
| 0.07 | 0.09 | 0.26 | 0.33 | 0.14 | 0.11 | 0.76 | 0.08 | 0.07 | 0.09 | 0.13 | |
| 0.09 | 0.18 | 0.02 | 0.02 | 0.07 | 0.03 | 0.05 | 0.13 | 0.02 | 0.03 | 0.01 | |
| 1445 | 1597 | 539 | 960 | 1698 | 1776 | 1736 | 1684 | 1832 | 2045 | 1429 | |
| 721 | 814 | 272 | 368 | 807 | 835 | 888 | 866 | 1007 | 1046 | 634 | |
| 22 | 75 | 89 | 34 | 106 | 24 | 139 | 213 | 40 | 42 | 21 | |
| 75 | 78 | 68 | 71 | 94 | 79 | 143 | 82 | 81 | 78 | 95 | |
| 169 | 166 | 248 | 214 | 188 | 263 | 322 | 295 | 184 | 230 | 300 | |
| 14 | 13 | 19 | 19 | 16 | 21 | 24 | 23 | 16 | 16 | 27 | |
| 48 | 41 | 65 | 56 | 40 | 95 | 118 | 100 | 48 | 56 | 110 | |
| 0.32 | 0.33 | 0.4 | 0.33 | 0.3 | 0.62 | 0.88 | 0.75 | 0.47 | n.a. | n.a. | |
| 5.2 | 4.87 | 7.36 | 6.9 | 4.15 | 8.66 | 11.22 | 9.73 | 4.75 | n.a. | n.a. | |
| 5.69 | 4.84 | 6.20 | 5.84 | 4.15 | 5.38 | 9.98 | 7.47 | 7.12 | n.a. | n.a. | |
| 14.16 | 12.10 | 16.50 | 15.27 | 9.74 | 14.91 | 24.12 | 19.60 | 14.48 | n.a. | n.a. | |
| 2.11 | 1.82 | 2.51 | 2.34 | 1.46 | 2.39 | 3.57 | 2.91 | 1.89 | n.a. | n.a. | |
| 8.90 | 7.90 | 11.15 | 10.56 | 6.65 | 11.43 | 15.68 | 13.52 | 7.86 | n.a. | n.a. | |
| 2.08 | 2.02 | 2.85 | 2.65 | 1.91 | 3.21 | 4.34 | 3.53 | 2.09 | n.a. | n.a. | |
| 0.63 | 0.61 | 1.17 | 1.08 | 0.81 | 0.95 | 1.29 | 1.22 | 0.77 | n.a. | n.a. | |
| 2.21 | 2.20 | 3.03 | 2.88 | 2.39 | 3.84 | 4.94 | 4.11 | 2.49 | n.a. | n.a. | |
| 2.37 | 2.43 | 3.10 | 3.02 | 2.46 | 3.93 | 5.00 | 4.11 | 2.61 | n.a. | n.a. | |
| 0.39 | 0.39 | 0.51 | 0.49 | 0.42 | 0.65 | 0.86 | 0.67 | 0.43 | n.a. | n.a. | |
| 0.51 | 0.52 | 0.68 | 0.66 | 0.55 | 0.81 | 1.06 | 0.87 | 0.57 | n.a. | n.a. | |
| 1.40 | 1.44 | 1.84 | 1.76 | 1.43 | 2.26 | 2.84 | 2.38 | 1.52 | n.a. | n.a. | |
| 0.21 | 0.22 | 0.28 | 0.26 | 0.21 | 0.31 | 0.42 | 0.34 | 0.22 | n.a. | n.a. | |
| 1.34 | 1.34 | 1.72 | 1.70 | 1.30 | 1.99 | 2.44 | 2.25 | 1.31 | n.a. | n.a. | |
| 0.22 | 0.21 | 0.28 | 0.27 | 0.19 | 0.31 | 0.38 | 0.32 | 0.20 | n.a. | n.a. | |
| 0.33 | 0.38 | 0.19 | 0.24 | 1.18 | 1.24 | 1.27 | 1.29 | 1.50 | n.a. | 0.12 | |
| 2.55 | 2.70 | 1.05 | 1.58 | 3.03 | 3.46 | 3.05 | 3.03 | 3.41 | n.a. | 2.31 | |
| 1.18 | 1.34 | 0.79 | 0.90 | 0.95 | 0.97 | 0.94 | 0.97 | 1.05 | n.a. | 0.27 | |
| 9.37 | 9.39 | 9.53 | 8.51 | 11.21 | 12.10 | 12.72 | 12.04 | 11.70 | n.a. | 13.01 | |
| 13.61 | 14.12 | 18.00 | 14.58 | 12.17 | 15.90 | 17.60 | 17.40 | 7.34 | n.a. | 15.91 | |
| 2.07 | 3.76 | 2.04 | 1.43 | 1.71 | 6.23 | 1.96 | 2.44 | 1.50 | n.a. | 0.39 | |

Ran HM	Ran LM	Ran LM									
Pirilä	Harjula	Harjula									
PR01-1	PR02-1	PR03-1	PR04-1	PR05-1	PR06-1	PR07-1	PR08-1	PR09-1	PR10-1	HJ1-1	HJ2-1
47.72	45.28	39.57	48.73	42.40	41.09	44.84	46.95	41.15	40.23	49.33	50.91
1.00	0.86	0.52	0.87	1.16	1.93	0.80	1.49	0.82	1.39	1.12	1.17
14.18	14.59	5.97	13.69	16.86	16.21	13.07	12.73	7.36	11.37	13.71	14.00
12.26	11.58	11.91	11.50	13.78	17.19	13.63	15.47	11.92	14.75	14.11	13.19
0.21	0.18	0.17	0.17	0.21	0.26	0.21	0.24	0.19	0.19	0.23	0.21
7.89	11.77	19.19	9.68	10.06	8.97	13.63	9.83	20.94	18.92	7.28	5.72
11.42	10.90	14.06	10.46	9.07	8.76	9.23	8.97	10.80	6.87	9.74	10.65
2.93	1.80	0.03	2.83	1.89	2.30	2.34	2.42	0.30	0.55	2.32	2.21
0.29	0.23	0.02	0.12	1.45	0.50	0.09	0.10	0.13	0.16	0.59	0.24
0.02	0.01	1.89	0.03	0.01	0.01	0.02	0.01	0.04	0.02	0.03	0.09
483	362	2169	462	670	326	358	372	2549	2763	117	124
228	306	892	320	195	170	501	240	1552	1265	85	89
131	25	117	41	53	26	41	70	38	22	50	199
82	83	653	98	98	132	95	104	91	189	109	96
271	220	129	223	319	364	202	292	173	229	318	328
19	17	10	15	20	36	15	29	12	15	22	25
46	45	27	47	51	117	49	86	44	84	64	71
0.21	0.28	0.11	0.26	n.a.	0.66	0.25	0.5	0.32	0.57	0.44	0.45
3.41	3.69	2.65	3.67	n.a.	9.11	3.4	7.14	4.32	8.32	4.61	4.8
3.34	3.60	1.28	3.42	n.a.	8.14	3.27	6.34	3.84	5.09	5.19	5.40
8.42	8.93	3.93	8.59	n.a.	20.63	8.18	15.94	8.61	12.36	12.58	13.41
1.34	1.38	0.66	1.36	n.a.	3.25	1.27	2.51	1.28	1.84	1.97	2.04
6.41	6.31	3.34	6.41	n.a.	15.34	5.96	11.60	5.82	8.30	9.05	9.42
2.10	2.03	0.99	1.96	n.a.	4.69	1.86	3.53	1.69	2.37	2.77	2.87
1.04	1.16	0.29	0.93	n.a.	1.69	0.68	1.42	0.56	0.85	1.12	1.12
2.84	2.47	1.27	2.60	n.a.	5.81	2.33	4.41	2.02	2.67	3.51	3.65
3.05	2.76	1.35	2.78	n.a.	6.39	2.56	4.77	2.11	2.62	3.94	4.12
0.50	0.45	0.22	0.46	n.a.	1.05	0.43	0.78	0.34	0.45	0.66	0.68
0.67	0.61	0.30	0.63	n.a.	1.44	0.58	1.07	0.44	0.57	0.90	0.94
1.86	1.61	0.80	1.64	n.a.	3.80	1.53	2.91	1.21	1.48	2.45	2.55
0.27	0.24	0.11	0.24	n.a.	0.56	0.23	0.45	0.18	0.22	0.38	0.40
1.60	1.46	0.72	1.43	n.a.	3.42	1.36	2.70	1.06	1.30	2.28	2.40
0.26	0.24	0.11	0.23	n.a.	0.54	0.23	0.43	0.16	0.22	0.37	0.37
0.22	0.14	2.00	0.22	n.a.	0.17	0.21	0.15	2.09	1.97	0.35	0.31
0.94	0.41	4.11	0.56	n.a.	0.54	0.45	0.50	4.65	4.94	0.25	0.22
0.88	0.15	1.02	0.21	n.a.	0.13	0.10	0.11	1.23	1.58	1.28	1.11
12.72	1.48	8.85	2.90	n.a.	2.22	1.35	1.72	11.86	18.14	17.91	15.50
18.38	1.95	9.76	3.13	n.a.	2.10	1.25	1.70	10.59	13.03	19.70	19.00
4.12	1.61	2.36	7.45	n.a.	0.42	1.55	1.87	7.99	2.24	1.04	1.98

Ran LM	Ran LM	Ran LM	Ran LM	Ran LM	Ran LM	Ran LM					
Harjula	Harjula	Harjula	Harjula	Harjula	Häsvuori	Häsvuori	Häsvuori	Kivelä	Kivelä	Kivelä	Kivelä
HJ3-1	HJ4-1	HV1-4	KK1-1	MK-1	HV1-1	HV1-2	HV1-3	KV1-1	KV1-1	KV1-1	KV1-2
49.35	48.78	48.70	48.47	48.28	47.95	46.23	49.37	48.16	48.16	47.26	
1.19	1.20	0.95	1.13	1.16	0.94	1.00	0.94	0.93	0.93	1.01	
14.26	14.19	14.15	14.32	14.45	13.97	14.86	14.48	14.49	14.49	15.27	
13.75	13.96	12.60	13.32	13.93	12.37	13.82	12.24	12.92	12.92	13.26	
0.20	0.22	0.18	0.21	0.22	0.19	0.20	0.17	0.18	0.18	0.19	
7.57	6.97	7.94	7.41	8.13	7.96	8.42	8.07	7.71	7.71	8.85	
10.50	10.66	11.19	10.16	10.49	12.17	11.52	10.16	12.34	12.34	10.55	
2.01	2.24	2.49	3.03	2.72	2.19	2.33	3.03	2.02	2.02	2.43	
0.14	0.25	0.43	0.28	0.16	0.18	0.28	0.17	0.11	0.11	0.21	
0.02	0.04	0.03	0.05	0.01	0.06	0.15	0.02	0.02	0.02	0.02	
125	120	187	115	102	189	192	184	157	157	162	
91	86	103	87	88	103	111	95	120	120	121	
128	127	81	28	47	132	161	45	88	88	98	
98	105	87	94	101	79	90	76	93	93	97	
326	332	287	319	329	288	327	289	280	280	303	
26	26	20	23	26	24	27	19	22	22	24	
62	71	50	63	66	52	56	53	46	46	49	
0.39	n.a.	0.26	0.37	n.a.	n.a.	0.26	0.26	0.27	0.27	n.a.	
4.66	n.a.	3.46	4.61	n.a.	n.a.	3.46	3.4	3.79	3.79	n.a.	
4.73	n.a.	4.26	4.86	n.a.	n.a.	4.16	3.92	3.90	3.90	n.a.	
12.24	n.a.	10.53	12.28	n.a.	n.a.	10.89	10.09	9.59	9.59	n.a.	
1.93	n.a.	1.64	1.94	n.a.	n.a.	1.75	1.60	1.45	1.45	n.a.	
8.92	n.a.	7.87	9.23	n.a.	n.a.	8.44	7.60	6.79	6.79	n.a.	
2.75	n.a.	2.48	2.92	n.a.	n.a.	2.76	2.38	2.16	2.16	n.a.	
1.13	n.a.	1.00	0.96	n.a.	n.a.	1.00	1.16	0.95	0.95	n.a.	
3.63	n.a.	3.19	3.73	n.a.	n.a.	3.58	3.11	2.88	2.88	n.a.	
4.08	n.a.	3.62	4.25	n.a.	n.a.	4.09	3.52	3.60	3.60	n.a.	
0.66	n.a.	0.59	0.69	n.a.	n.a.	0.68	0.58	0.57	0.57	n.a.	
0.91	n.a.	0.79	0.95	n.a.	n.a.	0.92	0.80	0.83	0.83	n.a.	
2.51	n.a.	2.19	2.58	n.a.	n.a.	2.53	2.13	2.34	2.34	n.a.	
0.39	n.a.	0.32	0.39	n.a.	n.a.	0.38	0.31	0.37	0.37	n.a.	
2.32	n.a.	1.94	2.35	n.a.	n.a.	2.24	1.87	2.18	2.18	n.a.	
0.37	n.a.	0.31	0.37	n.a.	n.a.	0.36	0.31	0.36	0.36	n.a.	
0.37	n.a.	0.28	0.47	0.40	n.a.	0.30	0.28	0.16	0.16	n.a.	
0.26	n.a.	0.24	0.31	0.31	n.a.	0.24	0.24	0.31	0.31	n.a.	
1.41	n.a.	0.97	1.18	0.84	n.a.	0.96	0.91	1.14	1.14	n.a.	
19.60	n.a.	18.00	21.00	35.91	n.a.	16.70	16.45	19.20	19.20	n.a.	
20.50	n.a.	15.50	24.40	15.81	n.a.	18.90	17.80	19.50	19.50	n.a.	
3.74	n.a.	2.16	10.29	2.48	n.a.	3.91	1.86	1.91	1.91	n.a.	

Ran LM	Ran LM	Ran LM	Ran LM	Ran LM	Ran LM	Ran LM	Ran LM	Ran LM	Ran LM
Kukonkivi	Kukonkivi	Kukonkivi	Pajulam-pi	Pajulam-pi	Parkumäki	Parkumäki	Porttiaho	Porttiaho	Porttiaho
KK1-2	MK-2	MK-3	PA1-1	PA1-2	PK1-1	PK1-2	Porttiaho 1	Porttiaho 2	Porttiaho 3
49.93	49.40	47.89	46.30	46.68	51.37	45.29	45.72	49.71	49.12
1.08	1.13	1.11	1.25	1.21	0.49	0.64	1.39	2.30	2.31
13.54	14.55	13.99	15.54	15.30	18.58	16.63	9.23	13.53	13.54
12.62	13.07	13.33	13.79	13.52	6.48	10.60	12.30	12.69	13.00
0.20	0.21	0.21	0.19	0.20	0.12	0.17	0.20	0.22	0.21
7.22	7.78	7.70	7.08	7.57	5.07	8.32	14.19	4.09	4.46
10.13	10.13	12.39	12.30	11.27	11.84	12.79	10.39	11.32	11.14
3.07	3.04	2.00	1.98	2.43	4.20	1.53	1.63	3.94	3.70
0.24	0.15	0.17	0.21	0.21	0.12	0.10	1.59	0.66	0.33
0.01	0.01	0.03	0.03	0.03	0.07	0.74	0.02	0.05	0.29
111	102	108	354	384	329	299	1261	23	46
83	91	84	240	267	68	54	195	29	15
14	29	79	123	123	18	103	32	43	105
88	98	96	86	90	49	78	114	158	170
315	298	320	257	256	181	234	250	447	391
23	22	24	22	21	17	17	26	49	46
64	67	63	58	49	30	60	227	179	194
0.31	n.a.	n.a.	0.79	0.8	0.48	0.67	8.14	1.14	1.43
4.5	n.a.	n.a.	10.3	10.36	3.47	5.58	20.18	13.86	15.68
4.62	n.a.	n.a.	5.82	5.98	5.11	7.36	42.82	14.98	16.06
11.90	n.a.	n.a.	14.30	14.69	11.20	16.28	93.78	36.60	38.24
1.88	n.a.	n.a.	2.21	2.21	1.49	2.22	14.42	5.32	5.86
9.09	n.a.	n.a.	9.72	10.22	6.10	9.14	58.69	24.08	25.90
2.83	n.a.	n.a.	2.94	2.98	1.50	2.16	11.98	6.78	7.16
1.15	n.a.	n.a.	1.26	1.29	0.64	0.75	3.45	2.29	2.55
3.58	n.a.	n.a.	3.68	3.69	1.83	2.42	9.91	8.29	8.56
4.02	n.a.	n.a.	4.18	4.20	2.17	2.86	6.48	8.82	9.33
0.67	n.a.	n.a.	0.66	0.68	0.34	0.44	1.37	1.38	1.56
0.89	n.a.	n.a.	0.93	0.94	0.52	0.67	1.17	1.84	2.05
2.44	n.a.	n.a.	2.53	2.61	1.43	1.86	2.69	5.16	5.54
0.38	n.a.	n.a.	0.38	0.40	0.24	0.30	0.36	0.78	0.84
2.21	n.a.	n.a.	2.41	2.44	1.48	1.91	2.04	4.85	5.06
0.35	n.a.	n.a.	0.38	0.39	0.25	0.33	0.31	0.73	0.82
0.40	0.41	0.40	0.14	0.07	0.07	0.08	0.30	n.a.	
0.25	0.32	0.30	0.78	0.56	0.31	0.24	0.15	n.a.	0.13
1.05	0.79	0.73	0.64	0.63	0.67	0.66	0.45	n.a.	0.04
17.40	33.22	28.61	4.27	4.24	11.16	11.74	6.19	0.19	0.45
20.90	16.47	21.65	15.90	16.10	18.40	16.90	7.91	0.08	0.33
1.58	3.35	8.02	2.36	2.45	2.21	1.54	2.07	3.11	2.42

| Ran LM |
|---------------|---------------|---------------|---------------|---------------|---------------|---------------|---------------|---------------|---------------|
| Savonlinna KH | Savonlinna RC | Savonlinna RC | Savonlinna RC |
| MS-1 | MS-2 | MS-3 | SC1-1 | SC2-1 | SC2-2 | SC3-1 | SRC1-1 | SRC1-2 | SRC1-3 |
| 49.58 | 53.18 | 63.97 | 48.91 | 51.45 | 51.26 | 53.25 | 51.52 | 51.43 | 51.68 |
| 1.90 | 1.38 | 0.53 | 1.67 | 1.62 | 1.64 | 1.44 | 1.67 | 1.37 | 1.65 |
| 13.92 | 14.27 | 15.19 | 13.61 | 12.51 | 13.26 | 14.91 | 14.91 | 14.08 | 14.15 |
| 13.79 | 11.61 | 7.00 | 13.75 | 13.66 | 13.45 | 10.52 | 13.01 | 12.39 | 13.68 |
| 0.19 | 0.17 | 0.08 | 0.19 | 0.16 | 0.17 | 0.07 | 0.12 | 0.15 | 0.13 |
| 5.56 | 4.79 | 2.76 | 5.58 | 5.62 | 5.60 | 4.94 | 6.00 | 4.64 | 5.60 |
| 10.42 | 8.65 | 4.07 | 12.04 | 8.81 | 8.53 | 8.79 | 7.72 | 7.97 | 8.21 |
| 3.56 | 2.97 | 3.90 | 2.48 | 3.05 | 3.42 | 2.20 | 2.19 | 2.55 | 1.93 |
| 0.46 | 0.91 | 1.62 | 0.51 | 1.26 | 1.11 | 1.88 | 1.26 | 2.37 | 1.49 |
| 0.09 | 0.34 | 0.12 | 0.22 | 0.07 | 0.07 | 0.10 | 0.06 | 0.81 | 0.03 |
| 113 | 111 | 59 | 136 | 124 | 160 | 303 | 125 | 114 | 128 |
| 72 | 86 | 36 | 69 | 82 | 83 | 130 | 67 | 57 | 66 |
| 144 | 190 | 57 | 265 | 63 | 59 | 80 | 82 | 175 | 47 |
| 122 | 128 | 96 | 106 | 124 | 117 | 134 | 144 | 200 | 131 |
| 377 | 340 | 83 | 355 | 330 | 360 | 260 | 329 | 303 | 337 |
| 28 | 25 | 27 | 28 | 27 | 26 | 25 | 27 | 28 | 26 |
| 115 | 104 | 145 | 97 | 93 | 95 | 122 | 111 | 102 | 109 |
| n.a. | n.a. | n.a. | 0.81 | 1.06 | n.a. | n.a. | 2.36 | 4.1 | n.a. |
| n.a. | n.a. | n.a. | 10.45 | 10.58 | n.a. | n.a. | 12.48 | 12.72 | n.a. |
| n.a. | n.a. | n.a. | 9.42 | 10.12 | n.a. | n.a. | 12.41 | 21.23 | n.a. |
| n.a. | n.a. | n.a. | 22.14 | 23.74 | n.a. | n.a. | 28.54 | 40.58 | n.a. |
| n.a. | n.a. | n.a. | 3.42 | 3.57 | n.a. | n.a. | 4.10 | 5.39 | n.a. |
| n.a. | n.a. | n.a. | 15.16 | 15.60 | n.a. | n.a. | 16.97 | 20.92 | n.a. |
| n.a. | n.a. | n.a. | 4.11 | 4.19 | n.a. | n.a. | 4.27 | 4.84 | n.a. |
| n.a. | n.a. | n.a. | 1.59 | 1.61 | n.a. | n.a. | 1.51 | 1.46 | n.a. |
| n.a. | n.a. | n.a. | 4.80 | 4.83 | n.a. | n.a. | 4.71 | 5.14 | n.a. |
| n.a. | n.a. | n.a. | 5.05 | 5.07 | n.a. | n.a. | 4.86 | 4.95 | n.a. |
| n.a. | n.a. | n.a. | 0.85 | 0.87 | n.a. | n.a. | 0.82 | 0.85 | n.a. |
| n.a. | n.a. | n.a. | 1.10 | 1.10 | n.a. | n.a. | 1.04 | 1.09 | n.a. |
| n.a. | n.a. | n.a. | 2.95 | 2.98 | n.a. | n.a. | 2.78 | 2.89 | n.a. |
| n.a. | n.a. | n.a. | 0.45 | 0.46 | n.a. | n.a. | 0.42 | 0.46 | n.a. |
| n.a. | n.a. | n.a. | 2.59 | 2.73 | n.a. | n.a. | 2.62 | 2.71 | n.a. |
| n.a. | n.a. | n.a. | 0.42 | 0.43 | n.a. | n.a. | 0.41 | 0.45 | n.a. |
| 0.11 | 0.15 | 0.08 | 0.15 | 0.10 | n.a. | n.a. | 0.12 | 0.14 | n.a. |
| 0.27 | 0.30 | 0.15 | 0.23 | 0.16 | n.a. | n.a. | 0.20 | 0.22 | n.a. |
| 0.43 | 0.51 | 0.06 | 0.65 | 0.43 | n.a. | n.a. | 0.55 | 0.56 | n.a. |
| 17.84 | 16.16 | 1.74 | 9.29 | 6.83 | n.a. | n.a. | 8.50 | 8.78 | n.a. |
| 21.21 | 16.95 | 1.38 | 14.20 | 12.13 | n.a. | n.a. | 11.61 | 13.88 | n.a. |
| 0.97 | 0.16 | 0.35 | 1.81 | 5.99 | n.a. | n.a. | 2.75 | 4.80 | n.a. |

Vam HM	Vam HM	Vam HM	Vam HM					
Kantoloppi	Kantoloppi	Kantoloppi	Kantoloppi	Kantoloppi	Komeron-lahti	Komeron-lahti	Komeron-lahti	Komeron-lahti
kantoloppi 1	kantoloppi 1	kantoloppi 2	kantoloppi 2	kantoloppi 3	K118.00	K14.00	K152.00	K170.00
44.72	44.56	39.02	38.89	44.14	46.60	46.33	45.49	45.66
0.81	0.80	0.87	0.87	0.81	0.84	1.02	1.71	1.55
8.83	8.72	12.70	12.61	8.38	8.37	9.45	7.78	10.27
11.72	11.64	12.32	12.29	10.94	12.93	12.64	14.32	14.70
0.18	0.18	0.18	0.18	0.19	0.18	0.20	0.23	0.20
21.23	21.08	19.72	19.65	20.36	22.07	21.27	18.90	14.79
7.87	7.82	7.11	7.09	8.43	7.94	8.45	11.18	11.57
0.64	0.66	0.48	0.48	0.36	0.87	1.42	1.03	1.24
0.16	0.16	0.63	0.63	0.17	1.12	0.13	0.34	1.04
0.41	0.40	0.03	0.03	0.03	n.a.	n.a.	n.a.	n.a.
1839	1845	2444	2438	2012	1916	1847	1642	1574
965	953	1509	1508	1120	804	448	453	244
41	50	31	32	70	n.a.	n.a.	n.a.	n.a.
87	88	126	128	78	n.a.	n.a.	n.a.	n.a.
188	201	200	206	192	213	240	285	270
13	16	14	13	14	n.a.	n.a.	n.a.	n.a.
45	46	44	43	46	n.a.	n.a.	n.a.	n.a.
0.36	0.36	0.29	0.29	0.35	n.a.	n.a.	n.a.	n.a.
4.9	4.9	4.9	4.9	4.7	n.a.	n.a.	n.a.	n.a.
4.38	4.38	4.01	4.01	4.36	n.a.	n.a.	n.a.	n.a.
10.74	10.74	9.04	9.04	10.85	n.a.	n.a.	n.a.	n.a.
1.55	1.55	1.31	1.31	1.62	n.a.	n.a.	n.a.	n.a.
7.32	7.32	6.14	6.14	7.64	n.a.	n.a.	n.a.	n.a.
1.97	1.97	1.76	1.76	2.03	n.a.	n.a.	n.a.	n.a.
0.64	0.64	0.63	0.63	0.67	n.a.	n.a.	n.a.	n.a.
2.40	2.40	2.24	2.24	2.50	n.a.	n.a.	n.a.	n.a.
2.52	2.52	2.32	2.32	2.50	n.a.	n.a.	n.a.	n.a.
0.40	0.40	0.37	0.37	0.42	n.a.	n.a.	n.a.	n.a.
0.52	0.52	0.48	0.48	0.52	n.a.	n.a.	n.a.	n.a.
1.49	1.49	1.36	1.36	1.50	n.a.	n.a.	n.a.	n.a.
0.21	0.21	0.19	0.19	0.21	n.a.	n.a.	n.a.	n.a.
1.36	1.36	1.18	1.18	1.36	n.a.	n.a.	n.a.	n.a.
0.20	0.20	0.17	0.17	0.20	n.a.	n.a.	n.a.	n.a.
1.37	1.37	2.46	2.46	1.51	n.a.	n.a.	n.a.	n.a.
3.60	3.60	4.96	4.96	3.93	n.a.	n.a.	n.a.	n.a.
0.96	0.96	1.18	1.18	1.10	n.a.	n.a.	n.a.	n.a.
9.14	9.14	11.70	11.70	10.80	n.a.	n.a.	n.a.	n.a.
10.80	10.80	11.40	11.40	11.80	n.a.	n.a.	n.a.	n.a.
1.61	1.61	12.70	12.70	10.50	n.a.	n.a.	n.a.	n.a.

Vam HM	Vam HM	Vam HM	Vam HM	Vam HM	Vam HM	Vam HM	Vam HM	Vam HM
Komeron-lahti	Komeron-lahti	Komeron-lahti	Ruotsila	Ruotsila	Ruotsila	Ruotsila	Ruotsila	Stormi
K80.00	K93.00	VMKML-24	R320-21.90	R320-35.32	R336-25.90	R336-44.25	R336-57.61	stormi 1
45.80	45.48	44.26	44.33	45.23	47.23	44.40	43.16	48.50
0.68	0.73	0.85	0.71	0.63	0.73	0.69	0.92	0.85
9.04	9.02	7.46	8.53	7.40	8.50	7.63	8.69	2.61
12.62	12.70	12.00	11.56	10.93	11.93	11.60	12.00	7.97
0.19	0.19	0.18	0.14	0.16	0.19	0.18	0.18	0.17
23.83	23.33	20.51	23.54	21.41	22.67	21.27	21.42	17.98
7.87	8.34	8.58	5.77	8.40	4.77	8.11	7.24	17.64
0.78	1.00	0.70	0.65	0.33	0.65	0.39	0.39	0.14
0.10	0.13	0.10	0.10	0.06	0.10	0.09	0.10	0.02
n.a.	n.a.	0.02	0.31	0.14	0.46	0.15	0.47	0.01
2053	1984	1460	1939	1417	1679	1838	2091	3395
1015	733	885	1035	1017	933	1125	981	379
n.a.	n.a.	28	73	66	34	81	69	9
n.a.	n.a.	70	74	54	75	57	67	52
207	203	162	203	175	189	182	208	153
14	16	14	12	15	14	10	14	9
33	41	53	44	35	50	41	53	37
0.6	0.8	1.1	0.3	0.28	0.29	0.33	0.4	0.41
5.5	5	12.1	4.2	3.8	4.4	4	5.5	5.6
4.00	5.20	11.46	3.25	3.54	3.19	4.78	4.78	5.81
9.80	12.50	23.90	7.94	9.38	7.87	10.83	12.21	13.99
1.50	1.80	3.00	1.13	1.44	1.12	1.54	1.75	2.07
6.60	7.80	12.08	5.51	6.87	5.35	6.99	8.22	9.76
2.00	2.30	2.49	1.52	1.79	1.51	1.75	2.30	2.46
0.80	0.90	1.00	0.38	0.83	0.41	0.60	0.79	0.81
2.70	2.90	2.42	1.92	2.06	1.84	2.09	2.71	2.50
3.10	3.40	2.11	2.07	2.12	1.97	2.13	2.71	1.77
n.a.	n.a.	0.36	0.33	0.35	0.32	0.35	0.44	0.35
n.a.	n.a.	0.41	0.43	0.44	0.41	0.45	0.55	0.30
1.80	2.10	1.14	1.28	1.31	1.22	1.31	1.59	0.73
n.a.	n.a.	0.16	0.18	0.19	0.18	0.19	0.22	0.09
1.60	1.90	1.02	1.17	1.24	1.17	1.21	1.44	0.56
n.a.	n.a.	0.15	0.17	0.19	0.18	0.18	0.22	0.08
n.a.	n.a.	1.12	1.82	1.25	1.34	1.83	1.63	0.51
n.a.	n.a.	2.46	4.15	3.01	2.63	3.12	3.78	1.81
n.a.	n.a.	0.67	1.09	0.79	0.99	1.01	1.19	0.15
n.a.	n.a.	5.75	11.00	8.30	9.47	10.20	12.10	1.04
n.a.	n.a.	5.76	11.10	8.70	12.80	10.50	12.50	0.94
n.a.	n.a.	0.95	5.90	9.49	2.89	9.97	5.87	-0.01

Vam HM	Vam HM	Vam HM	Vam HM	Vam HM	Vam HM	Vam HM	Vam HM	Vam HM	Vam HM
Stormi	Stormi	Stormi	Stormi	Uusiniitty	Uusiniitty	Uusiniitty	Uusiniitty	Uusiniitty	Uusiniitty
stormi 2	stormi 3	stormi 4	TY179-125.50	TY193-31.80	U11.90	U147.00	U157.50	U16.00	U60.10
45.19	43.59	43.10	45.35	43.41	47.72	45.96	46.79	47.85	45.44
0.70	1.55	1.79	0.80	1.24	0.71	1.47	1.76	0.84	0.94
2.10	7.50	7.49	8.65	7.84	8.22	8.29	9.31	8.44	9.22
11.94	14.47	14.31	12.22	13.47	12.03	14.11	14.47	12.64	12.46
0.17	0.19	0.19	0.20	0.19	0.21	0.19	0.21	0.19	0.16
21.22	14.97	16.65	22.79	19.01	23.57	19.54	15.73	22.26	18.09
12.15	12.51	10.14	5.55	8.45	7.54	10.34	10.95	7.84	12.46
0.15	1.77	1.07	1.07	0.82	0.71	0.96	1.39	0.64	1.22
0.02	0.29	0.26	0.15	0.13	0.14	0.11	0.46	0.13	0.93
0.03	0.02	0.03	0.19	0.30	n.a.	n.a.	n.a.	n.a.	n.a.
2570	1667	1644	1935	1825	1916	1642	1300	2258	1916
731	802	816	829	979	279	603	598	647	710
23	143	207	72	114	n.a.	n.a.	n.a.	n.a.	n.a.
69	83	93	73	96	n.a.	n.a.	n.a.	n.a.	n.a.
139	228	239	199	205	203	274	314	220	223
6	17	18	15	13	15	n.a.	n.a.	15	n.a.
22	94	115	33	76	40	n.a.	n.a.	43	n.a.
0.27	1.56	1.66	0.15	1.18	1.1	n.a.	n.a.	0.7	n.a.
2.7	17.4	20.8	2.9	14.9	4.5	n.a.	n.a.	5.5	n.a.
4.66	12.88	17.37	1.93	12.65	5.60	n.a.	n.a.	4.90	n.a.
9.88	31.03	37.86	5.52	27.14	13.00	n.a.	n.a.	12.00	n.a.
1.43	4.19	4.96	0.92	3.48	1.90	n.a.	n.a.	1.90	n.a.
6.96	18.32	21.69	5.02	14.78	8.00	n.a.	n.a.	8.20	n.a.
1.82	4.09	4.78	1.59	3.29	2.40	n.a.	n.a.	2.70	n.a.
0.67	1.26	1.60	0.54	0.89	0.90	n.a.	n.a.	1.10	n.a.
1.86	4.14	4.73	2.08	3.41	3.00	n.a.	n.a.	3.30	n.a.
1.41	3.34	3.65	2.20	2.97	3.30	n.a.	n.a.	3.40	n.a.
0.26	0.61	0.70	0.34	0.52	n.a.	n.a.	n.a.	n.a.	n.a.
0.24	0.61	0.68	0.47	0.57	n.a.	n.a.	n.a.	n.a.	n.a.
0.60	1.63	1.76	1.31	1.56	2.00	n.a.	n.a.	2.00	n.a.
0.07	0.22	0.23	0.20	0.22	n.a.	n.a.	n.a.	n.a.	n.a.
0.44	1.35	1.45	1.20	1.37	1.90	n.a.	n.a.	1.80	n.a.
0.06	0.19	0.20	0.19	0.20	n.a.	n.a.	n.a.	n.a.	n.a.
2.72	1.56	1.52	1.11	1.40	n.a.	n.a.	n.a.	n.a.	n.a.
6.55	3.20	2.78	3.78	3.24	n.a.	n.a.	n.a.	n.a.	n.a.
0.41	1.03	0.86	1.10	1.00	n.a.	n.a.	n.a.	n.a.	n.a.
1.85	9.31	7.69	10.70	8.78	n.a.	n.a.	n.a.	n.a.	n.a.
1.73	8.54	7.59	34.50	9.03	n.a.	n.a.	n.a.	n.a.	n.a.
-0.01	1.51	9.07	1.73	6.34	n.a.	n.a.	n.a.	n.a.	n.a.

Vam HM	Vam HM	Vam HM	Vam HM	Vam HM	Vam HM	Vammala	Vammala	Vammala	Vammala	Vammala
Uusiniitty	Uusiniitty	Uusiniitty	Uusiniitty	Uusiniitty	V102.00	V110.0	V125.0	V54.00	V86.00	
U99.00	uusiniitty 1	uusiniitty 2	uusiniitty 3	uusiniitty 4c						
47.19	44.19	43.73	43.57	46.65	46.04	45.73	45.27	45.33	45.84	
0.83	0.72	0.79	0.83	0.86	0.73	0.87	0.77	0.82	0.76	
8.67	8.56	9.24	9.10	9.24	8.69	8.53	8.23	8.89	8.10	
13.39	11.97	12.28	11.63	11.38	12.63	12.86	13.32	13.23	12.90	
0.17	0.19	0.18	0.17	0.19	0.18	0.20	0.21	0.20	0.19	
19.90	21.13	21.01	17.80	17.62	23.16	23.61	23.80	23.24	24.41	
9.33	8.09	7.39	10.97	10.12	8.23	8.21	8.29	8.23	7.85	
1.35	0.35	0.43	1.10	0.87	1.02	0.80	0.99	0.75	0.71	
0.16	0.06	0.04	0.13	0.23	0.20	0.12	0.13	0.30	0.17	
n.a.	0.01	0.14	0.15	0.06	n.a.	n.a.	n.a.	n.a.	n.a.	
1916	1918	2107	2115	1508	2053	2121	2121	1916	2053	
1083	1010	1054	1090	773	969	1024	1078	1080	910	
n.a.	50	99	70	40	n.a.	n.a.	n.a.	n.a.	n.a.	
n.a.	71	96	71	65	n.a.	n.a.	n.a.	n.a.	n.a.	
230	198	201	206	217	202	222	217	218	209	
n.a.	13	12	14	12	n.a.	n.a.	10	n.a.	11	
n.a.	38	43	48	49	n.a.	n.a.	31	n.a.	40	
n.a.	0.33	0.43	0.4	0.42	n.a.	n.a.	0.4	n.a.	1.2	
n.a.	4.1	5	5.2	5.4	n.a.	n.a.	3	n.a.	5.5	
n.a.	4.02	4.48	4.15	5.72	n.a.	n.a.	2.30	n.a.	5.00	
n.a.	9.78	10.80	10.83	13.40	n.a.	n.a.	6.80	n.a.	11.60	
n.a.	1.43	1.59	1.61	1.86	n.a.	n.a.	1.30	n.a.	1.90	
n.a.	6.91	7.50	7.78	8.58	n.a.	n.a.	7.00	n.a.	8.60	
n.a.	1.93	2.07	2.15	2.27	n.a.	n.a.	2.70	n.a.	2.80	
n.a.	0.66	0.49	0.69	1.24	n.a.	n.a.	1.20	n.a.	1.20	
n.a.	2.21	2.41	2.64	2.60	n.a.	n.a.	3.50	n.a.	3.60	
n.a.	2.36	2.46	2.75	2.55	n.a.	n.a.	3.60	n.a.	3.60	
n.a.	0.37	0.40	0.45	0.42	n.a.	n.a.	n.a.	n.a.	n.a.	
n.a.	0.48	0.52	0.56	0.52	n.a.	n.a.	n.a.	n.a.	n.a.	
n.a.	1.38	1.49	1.62	1.49	n.a.	n.a.	2.20	n.a.	2.20	
n.a.	0.20	0.21	0.23	0.22	n.a.	n.a.	n.a.	n.a.	n.a.	
n.a.	1.28	1.38	1.45	1.39	n.a.	n.a.	2.40	n.a.	2.40	
n.a.	0.19	0.21	0.22	0.21	n.a.	n.a.	n.a.	n.a.	n.a.	
n.a.	1.45	1.56	1.74	1.17	n.a.	n.a.	n.a.	n.a.	n.a.	
n.a.	3.20	3.36	4.00	2.52	n.a.	n.a.	n.a.	n.a.	n.a.	
n.a.	1.02	1.09	1.04	0.85	n.a.	n.a.	n.a.	n.a.	n.a.	
n.a.	9.87	9.89	10.10	9.57	n.a.	n.a.	n.a.	n.a.	n.a.	
n.a.	9.04	10.90	12.10	10.90	n.a.	n.a.	n.a.	n.a.	n.a.	
n.a.	2.89	0.84	6.90	1.63	n.a.	n.a.	n.a.	n.a.	n.a.	

Table 4. Location and classification of metabasalt and metapicrite samples.

Study area	Locality	Geochemical Grouping	Number of samples
Juva area	Mustalampi	Rantasalmi High-Mg	4
	Porttiaho	Rantasalmi Low-Mg	3
Kestilä area	Kettukaarrot	Kestilä Low-Mg	2
	Ritokoski	Kestilä Low-Mg	2
Kiuruvesi area	Hallaperä	Pielavesi Low-Mg	3
Pielavesi area	Kärväjärvi	Pielavesi Low-Mg	5
	Koivujoki	Pielavesi Low-Mg	3
	Teerimäki	Pielavesi Low-Mg	3
	Kumpukangas	Kestilä Low-Mg	2
Rankinen area	Takukangas	Kestilä Low-Mg	5
	Tervahauta	Kestilä Low-Mg	2
Rantasalmi area	Pahakkala	Rantasalmi High-Mg	7
	Pajulampi	Rantasalmi Low-Mg	2
	Pirilä	Rantasalmi High-Mg	14
Savonlinna-Kerimäki area	Harjula	Rantasalmi Low-Mg	7
	Häsävuori	Rantasalmi Low-Mg	3
	Kivelä	Rantasalmi Low-Mg	2
	Kukonkivi	Rantasalmi Low-Mg	3
	Parkumäki	Rantasalmi Low-Mg	2
	Savonlinna Casino Hotel	Rantasalmi Low-Mg	7
Vammala area	Savonlinna Railway Cutting	Rantasalmi Low-Mg	3
	Stormi	Vammala High-Mg	6
	Uusiniitty	Vammala High-Mg	5
	Kantoloppi	Vammala High-Mg	3
	Ketola	Vammala High-Mg	3
	Komerolahti	Vammala High-Mg	1
	Ruotsila	Vammala High-Mg	6

gneisses runs 2–10 km north of the volcanic rocks. Near Savonlinna, mainly east of it, occurs a separate volcanic zone in cordierite gneiss. It is composed mainly of mica amphibolites with skarn bands (Gaál & Rauhamäki, 1971). Samples from Savonlinna Casino, Kivelä and Railway cut come from this zone.

3.2. Rantasalmi area

Harjula samples come from mafic volcanic rocks in the NW side of Haukivesi. They form a zone about

15 km long north of the Putkilahti gabbro-granodiorite pluton (c. 1.84 Ga, Vaasjoki & Kontoniemi, 1991). Most of the Rantasalmi area samples however have been taken from Pirilä and Pahakkala sites, which are composed of well preserved mafic to ultramafic volcanic rocks surrounded mainly by low amphibolite facies metaturbidites. 1.88 Ga tonalite bodies (Korsman et al., 1984; Vaasjoki & Kontoniemi, 1991) occur south and east of the volcanic rocks. The volcanic rocks have been described by Kousa (1985). Primary structures include pillows, pyroclastic brec-

cias and possibly also autobreccias. Stratigraphically, the ultramafic rocks overlay the mafic rocks. The mafic volcanic rocks in Pajulampi belong to the Viholanniemi–Lahnalahti felsic (1.906 Ga, Vaasjoki & Sakkö, 1988) to mafic volcanic complex (geology studied by e.g. Zhang, 2000). Pillow structures are well preserved in the mafic rocks.

3.3. Juva area

Sampling sites Mustalampi and Rantala belong to a NW–SE running c. 25 km long Narila volcanic zone, while Porttiaho samples come from a small separate lens of mafic volcanics. The volcanic rocks in the Juva area represent the younger volcanic episode in the area (1.89–1.88 Ga) where ultramafic lenses occur as well. Locally pillow lava structures are visible (Pekkarinen, 2002). The volcanic rocks are surrounded by mica gneiss or mica schist, the former being slightly older than the latter. The metamorphic grade of the sampling areas is medium amphibolite facies. Numerous small nickel occurrences are found east of the Narila volcanic zone. The Rantala target forms one of these nickel occurrences. There the ultramafic rock may represent a subvolcanic sill. The Rantala igneous body includes a gabbro component, which was also sampled.

3.4. Pielavesi area

Four localities were sampled: Kärväsijärvi, Teerimäki, Koivujoki and Kumpukangas. They all are situated within or near the youngest metasediments (mica-hornblende gneisses) of the Pielavesi area, called the Koivujoki suite by Ekdahl (1993). Sampled mafic and intermediate volcanic rocks occur as narrow intercalations in mica gneiss. Locally they exhibit pillow structures. Rocks of the Koivujoki suite have a lower metamorphic grade (medium amphibolite facies) than the older migmatites and volcanic rocks (1.92–1.90 Ga) east and west of the suite (upper amphibolite to granulite facies). The sampled volcanic rocks at the Teerimäki sampling site are located near the Teerimäki gabbro body.

3.5. Kiuruvesi area

The Kiuruvesi area represents a high-grade metamorphic terrain with numerous pyroxene granitoids (Hölttä, 1988). Many of the mafic volcanic rocks have been migmatised.

3.6. Kestilä area

The sampled mafic metavolcanic rocks at Kettukaarrot and Ritokoski occur as small separate lenses within the mica gneiss. At Ritokoski the rock is weakly altered. Although deformed, pillow lava structures are still recognizable. At Kettukaarrot the volcanic rocks contain disseminated pyrrhotite+pyrite.

3.7. Rankinen area

Between Rantsila and Vihanti there is an EW-trending, c. 20 km long zone of mafic volcanic rocks. Stratigraphically they overlie the surrounding mica gneisses (Rouhunkoski, 1968). Sampling sites Kumpukangas, Tervahauta and Takukangas are located in this zone. At Takukangas a small gabbro body occurs at the contact of the sampled volcanic rocks.

3.8. Vammala area

Six metapicritic formations were sampled from the Vammala area within the central part of the Vammala Nickel Belt: Stormi, Uusiniitty, Kantoloppi, Keto-la, Komeronlahti and Ruotsila. All these targets are located within a rather small area of c. 10 x 2 km. Picritic formations occur as strongly metamorphosed (upper amphibolite facies), discontinuous boudins within migmatitic metaturbidites which were deposited at c. 1.9–2.0 Ga. At Stormi these picritic rocks occur in intimate contact with ultramafic intrusions but in all other cases picritic formations occur as separate intercalations within metagraywackes. Primary structures are generally not preserved but pillow and flow breccia structures are locally evident. Detailed core logging at Uusiniitty suggests that metapicritic rocks alternate with amphibolites, skarns and

metapelites thus leaving little doubt about their supracrustal origin.

The present mineralogy in the picritic rocks is completely metamorphic consisting of olivine and orthopyroxene porphyroblasts in a matrix of fine-grained clinoamphibole, clinopyroxene and green spinel (hercynite).

4. Petrology and Geochemistry of the Metavolcanic Rocks

4.1. Lithologies

The mafic metavolcanic rocks are primarily exposed as complexly folded bands within the micaceous gneisses. They are typically pillow lavas showing widely varying degrees of deformation from mild to extreme. Lithologically they are predominantly hornblende amphibolites containing diopside, plagioclase, quartz, biotite, chlorite, carbonate and magnetite.

The metapicrite samples are porphyroblastic rocks composed of metamorphic olivine, serpentine, tremolite-actinolite, diopside, chlorite, hornblende, quartz, carbonate, magnetite, haematite and minor sulfide. No primary igneous mineralogy is retained. The most intensely deformed pillow sequences, such as those in the Savonlinna area, contain centimetre-scale *en echelon* bands of diopside-rich calc-silicate schist, probably representing patches of interpillow material transposed into the foliation. Care was taken during sampling to avoid these bands. Detailed petrographic description of all the samples is given in Hill et al. (2005).

4.2. Subdivision and major element geochemistry

The metavolcanic rocks have been divided into five suites, based on location and common geochemical characteristics summarised as follows:

Rantasalmi low-Mg suite (RLM): low-Mg tholeiite suite from the Rantasalmi and Savonlinna areas in the south-east part of the Kotalahti Belt, having tightly clustered major element compositions, predominantly chondritic to weakly enriched lithophile incompat-

ible trace element profiles with locally strong alteration overprint.

Rantasalmi high-Mg suite (RHM): high-Mg tholeiite/picrite suite with accumulated or transported phenocryst olivine, from the Pirilä, Pahakkala and Mustalampi localities in the Rantasalmi-Savonlinna-Juva area to the south-east of the Kotalahti Belt. These have similar trace element patterns to RLM.

Pielavesi low-Mg suite (PLM): fractionated low-Mg tholeiites with a strong alteration overprint, from the Pielavesi and Kiuruvesi areas in the central part of the Kotalahti Belt.

Kestilä low-Mg suite (KLM): mafic to intermediate pillow lavas from the Kestilä and Rankinen areas in the north-western part of the Kotalahti Belt.

Vammala high-Mg suite (VHM): High-Mg tholeiite/picrite suite with accumulated or transported phenocryst olivine from the Vammala Belt. The rocks have similar geochemical characteristics to RHM.

Major element characteristics of these suites are shown in Fig. 3. The RHM and VHM suites have similar compositions, and plot broadly along olivine control lines implying presence of variable proportions of phenocryst olivine. The RLM and the KLM suites show a high degree of similarity, and overlap the lower-Mg end of the RHM suite. The PLM suite is distinct from the others in having lower MgO and lower TiO₂ and FeO_{tot} and higher SiO₂ and Al₂O₃ for a given MgO content.

Figure 3 shows plots of model 2 kbar fractional crystallization trends for a hypothetical starting liquid composition based on a Rantasalmi High-Mg suite composition with 15 % MgO, calculated using the MELTS model (Ghiorso & Sack, 1995). The model predicts crystallization of olivine plus chromite from a liquidus temperature of 1380 °C down to 1240 °C where chromite is replaced by clinopyroxene, and appearance of liquidus plagioclase at around 1200 °C. The modeling is consistent with rocks of the RHM and VHM suites being derived largely as mixtures of olivine-saturated liquids with accumulated olivine. The more Mg-rich members of the RLM and KLM suites could be derived as low-pressure fractionates of the RHM parent. However, all three low-Mg suites

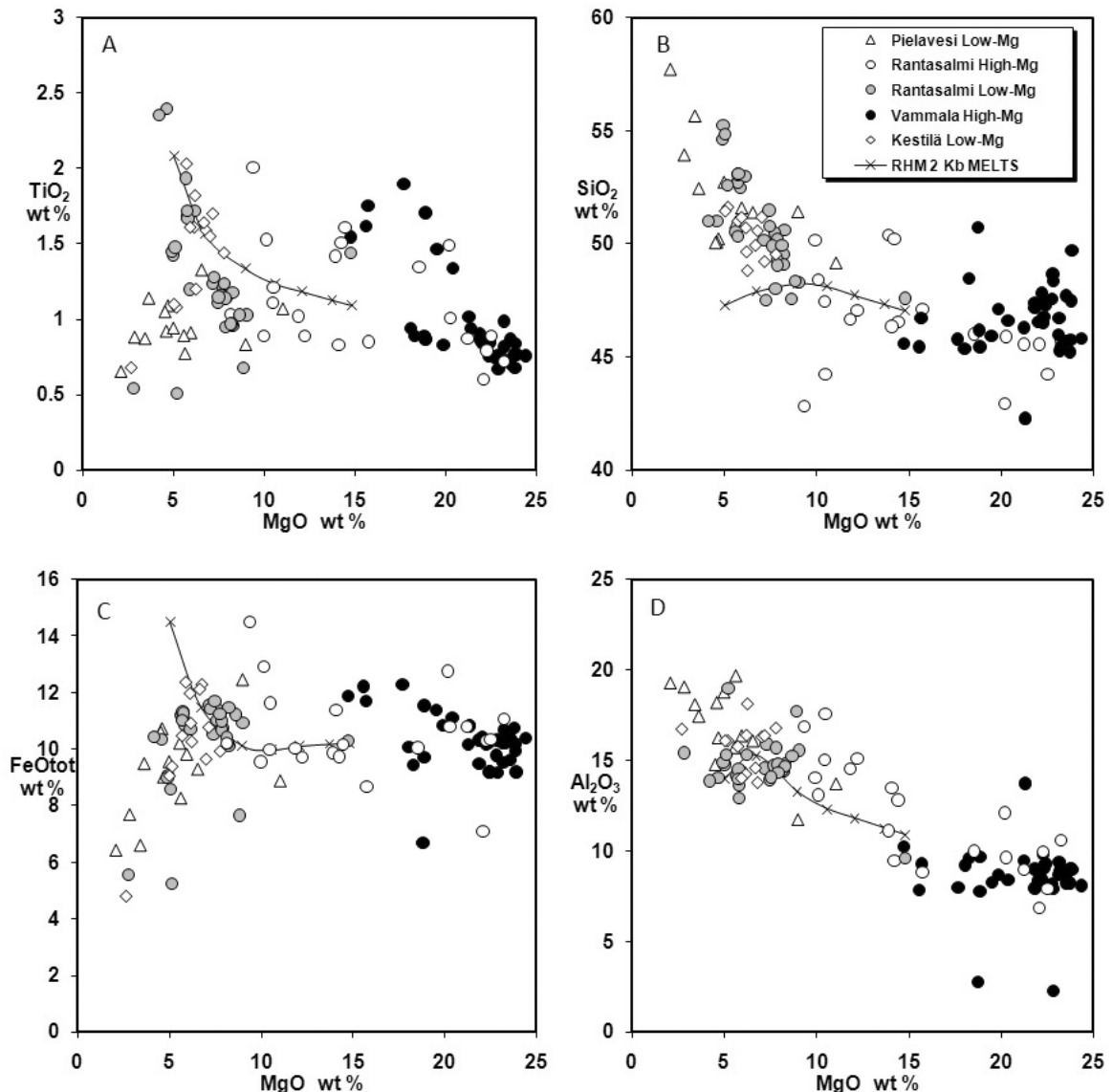


Fig. 3. Major element geochemistry: weight % of SiO_2 , TiO_2 , FeO_{TOT} and Al_2O_3 vs MgO , all analyses recalculated to 100 % volatile-free.

show trends of increasing silica with decreasing MgO which is at a sharp angle to the low-pressure fractionation curve (Fig. 3b). This can be interpreted in a number of ways: these suites have had their chemistry modified by silica metasomatism; their evolution has involved substantial contamination with siliceous crustal material during fractionation of an RHM-like parent; or they are completely independently derived

and owe high Si contents to partial melting under hydrous conditions. We return to these alternatives below.

4.3. Compatible trace element geochemistry

Plots of Ni and Cr vs. MgO (Fig. 4) also show a division between the Rantasalmi High-Mg suite sam-

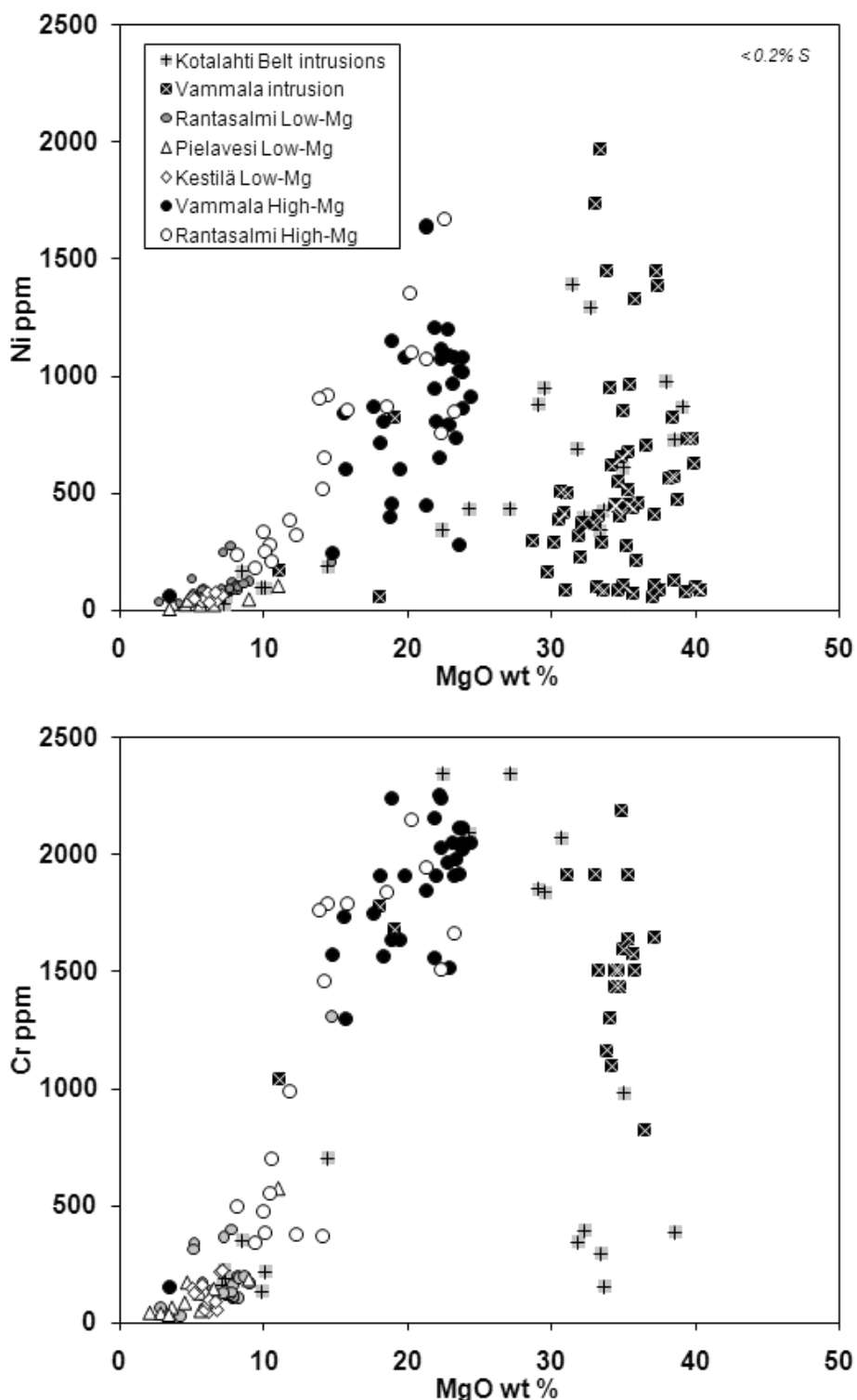


Fig. 4. Ni and Cr vs MgO for all volcanic suites and for samples from the intrusions in the Kotalahti and Vammala Belts (see text for data sources).

ples from Pirilä, Pahakkala and Mustalampi, and low Mg-suite rocks from elsewhere. The high Mg suites show positive correlation between MgO, Ni and Cr implying control by fractionation and accumulation of olivine, together with either pyroxene or chromite. Low Mg rocks show generally low and fairly similar Ni and Cr contents.

4.4. Incompatible trace element geochemistry

Median, 10th and 90th percentiles of immobile incompatible elements on samples from all suites are shown in Figure 5 as chondritic-normalized abundances. Variability within and between these various groups can also be seen on a series of primitive mantle-normalised ratio/ratio plots (Fig. 6). Statistics on chondritic-normalized ratios for the various volcanic groups, and the associated intrusive suites are given in Table 5.

Alteration has almost certainly modified incompatible element ratios and abundances, bearing in mind that all the samples analyzed have been extensively reconstituted during metamorphism. If alteration effects were important, they would be expected to produce wide ranges in abundances of mobile elements between samples from the same locality. Several of the Rantasalmi-Savonlinna area localities show wide variations of La and Th and compared with relatively consistent patterns in the heavy rare earths (Fig. 5c). Element mobility is seen particularly in the RLM samples of the Savonlinna area for La, Th and to a lesser extent Nb, where enrichment in these elements also correlates weakly with abundance of K, which varies widely (Table 3). This variance in K is most likely due to potassic alteration, as observed in thin section in the Savonlinna samples, and corresponding to the presence of small pegmatitic veins and dykes in this area. A similar observation applies to a lesser extent to the samples from Pahakkala in the RHM.

Quantification of these effects is impossible, but they have been minimised by excluding from the following discussion individual samples with >1 % K₂O and those with highly erratic trace element patterns.

Commonly, these features coincide in the same samples.

4.5. Interpretation of trace element data

The variance displayed within and between the different suites can be the result of four major processes: partial melting of a variable source; fractional crystallization and crystal accumulation; contamination by continental crust; and modification by metasomatic introduction of elements during metamorphism and alteration. Given the somewhat erratic chemical characteristics of all five suites, these processes are very difficult to distinguish from one another.

Considering the volcanic suites from the Kotalahti Belt, the Rantasalmi high-Mg and low-Mg suites are broadly similar to one another in most of the incompatible element ratios (Figs. 5 and 6; Table 5). The Kestilä and Pielavesi suites are slightly enriched in Gd/Yb (i.e. they have a steeper slope at HREE) compared with both Rantasalmi suites.

The primitive mantle normalised Zr/Yb and Gd/Yb ratios are significantly correlated within each suite, but show subtly different trends for different suites. The Rantasalmi low-Mg and high-Mg suites fall on the same trend, the Pielavesi suite is displaced to higher Gd/Yb, and the Kestilä suite is intermediate (Fig. 6a). The correlation is not likely to be entirely the result of alteration and can be explained either as the result of crustal contamination, or by partial melting of variably enriched source mantle. Given that the Rantasalmi low- and high-Mg suite samples are all from a restricted area, and that they represent mafic magmas emplaced within continental crust, a model involving variable degrees of crustal contamination with a component of postcrystallization metasomatic alteration is most reasonable. It is also consistent with the observation made above that the major element compositions of the low-Mg suites are incompatible with derivation from the high-Mg suites by simple fractional crystallization.

The most likely explanation is that the Rantasalmi high-Mg and low-Mg suites form a single coherent, comagmatic suite of lavas related by fractionation of

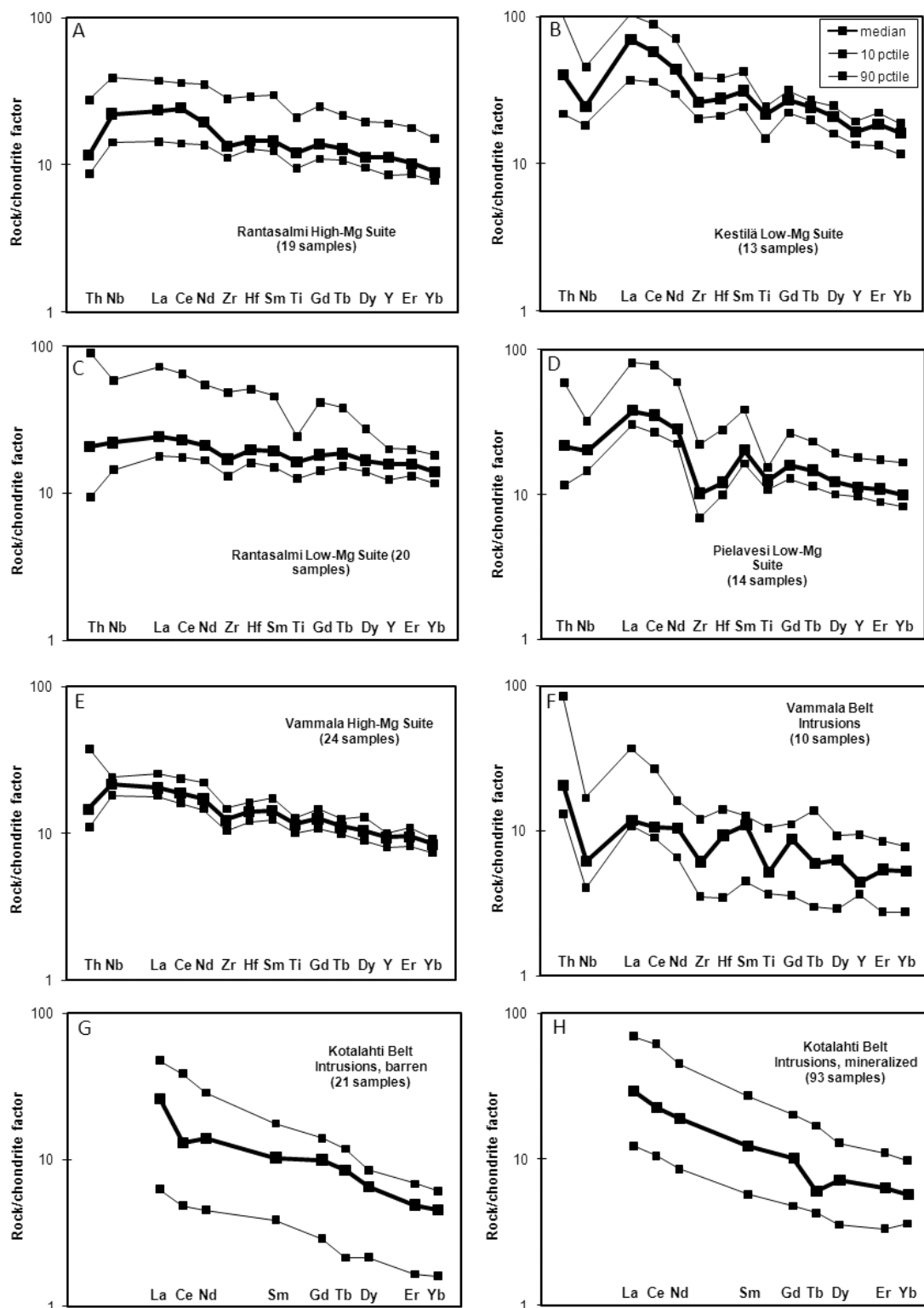


Fig. 5. Comparative statistics on incompatible trace element abundances (normalised to chondrite) in the various geochemical suites from the Kotalahti and Vammala Belts. All data shown as median, 10th and 90th percentiles over the given number of samples, excluding "altered" samples with $K_2O > 1.0\%$.

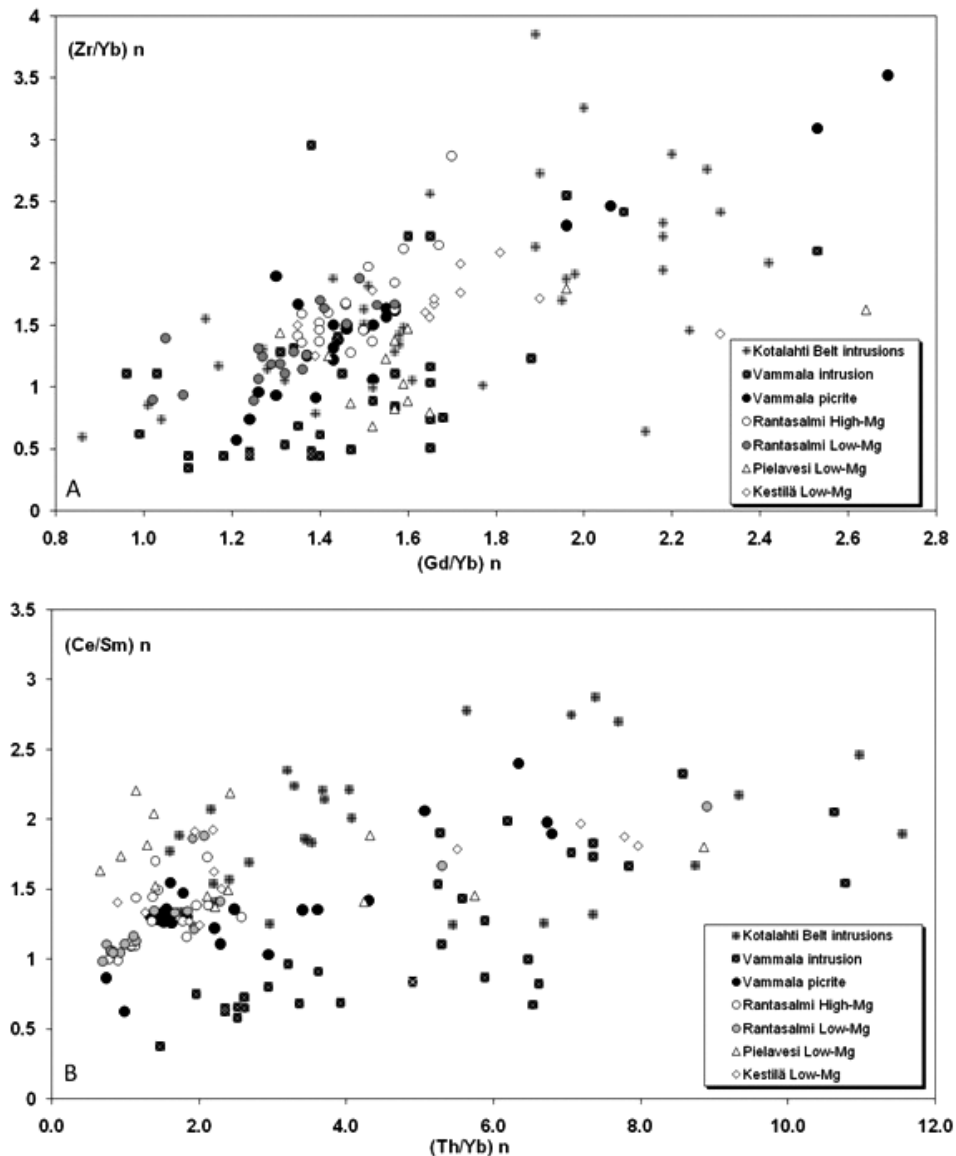


Fig. 6. Plot of primitive mantle-normalised incompatible element ratios for samples from volcanic suites and intrusions, excluding “altered” samples with $K_2O > 1.0\%$.

olivine and variable degrees of crustal contamination, with a superimposed imprint of alteration involving addition of silica. All of the Kotalahti belt lavas have a significantly lower Al/Ti relative to chondritic mantle (Table 5). Either the ratio has been modified by alteration, or it reflects variability in the mantle source (unlikely over such a small area), or variation in the degree of melting of a garnet-bearing source. The chemistry is further complicated by metasomatic mobility of LREE and possibly Th, accounting for

the wide variety of patterns seen in the multi-element plots in Figure 5. The Rantasalmi low-Mg suite appears to be the least contaminated in terms of incompatible trace element abundances.

It is likely that the Kestilä lavas belong to the same linear trend as the Rantasalmi suites. The combination of higher Gd/Yb, and distinct major element characteristics including high silica suggests that the Pielavesi lavas may represent a distinct magmatic lineage.

Table 5. Chondrite-normalised incompatible trace element ratios – average and standard deviation over number of samples plotted in Fig. 5. Normalising values from McDonough & Sun (1995).

Locality group	Kestilä Low-Mg		Kotalahti Belt intrusions		Pielavesi Low-Mg		Rantasalmi High-Mg		Rantasalmi Low-Mg		Vammala Intrusion		Vammala picrite	
Chond-norm ratio	median	sd	median	sd	median	sd	median	sd	median	sd	median	sd	median	sd
Ce/Sm	1.79	0.44	1.89	0.49	1.69	0.29	1.27	0.22	1.22	0.35	0.97	0.58	1.33	0.46
Gd/Yb	1.66	0.29	1.83	0.96	1.58	0.40	1.47	0.10	1.33	0.62	1.44	0.32	1.48	0.64
Zr/Yb	1.72	0.87	1.67	1.12	1.13	0.42	1.60	0.39	1.27	0.86	0.89	0.86	1.50	0.79
Al/Ti	0.43	0.21	0.69	0.37	0.81	0.23	0.50	0.15	0.55	0.34	0.69	0.17	0.49	0.20
Th/Yb	2.21	7.47	3.45	9.42	2.16	2.29	1.36	0.49	1.52	5.18	5.28	4.57	1.71	5.06
Th/Nb	1.79	1.81	No data		1.05	0.86	0.59	0.11	0.69	0.74	3.75	3.80	0.66	1.88
Zr/Ti	1.00	0.96	1.04	0.40	0.79	0.68	1.13	0.16	1.12	0.51	1.01	0.81	0.85	0.86
Pt/Ti	0.01	0.03	0.03	0.03	0.02	0.03	0.08	0.05	0.13	0.07	0.05	4.81	0.11	0.04
Pd/Ti	0.04	0.09	0.06	2.73	0.04	0.11	0.21	0.11	0.27	0.15	0.09	28.01	0.22	0.14

Turning to the Vammala picrite suite, despite the geographical separation there appear to be strong similarities with the Rantasalmi high-Mg suite, although some of the Vammala samples extend towards more primitive (low Ce/Sm, Th/Yb) compositions (Figs. 5e and 6a). The two suites are interpreted as being comagmatic, but with a superimposed metasomatic signature.

4.6. Petrogenetic affinities

The Pielavesi suite is notably depleted in Zr and slightly depleted in Nb as compared with the other Kotalahti Belt suites (Figs. 5 and 6; Table 5). These distinctive HFSE depletions, along with its high-Al character and variable silica content, strongly suggest that it is a subduction-related arc magma suite (Fig. 7). The other suites are probably at least of mutually similar affinity if not entirely comagmatic, and have predominantly chondritic mantle signatures, with a component of crustal contamination and alteration. Peltonen (1995b) interpreted the signatures of a smaller dataset of Vammala Belt picrites as being akin to transitional MORBs. The RHM, RLM, VHM suites could be of predominantly oceanic affinity, or could also be plume products. The similarity of the trend on the plot of Nb/La vs. Nb/Th to the typical range of values in continental flood basalt suites,

and the general shape of the multi-element patterns (Fig. 5; Table 5) is more consistent with a continental flood basalt affinity and hence a probable plume origin.

4.7. Relationship to intrusions

Makkonen (1996) concluded that the metapicrites are metabasalts containing abundant phenocrystic olivine and that the accumulation of olivine took place in flow conduits or during eruption. Similar nickel mineralization hosted by the Svecofennian intrusions is found in metapicrites at Juva and Rantasalmi and northwest of Mikkeli. Other geological evidence supporting the genetic relationship between the nickel-bearing intrusions and metapicrites is found in Juva area, where within a single, 4 km long, linear belt of nickel deposits the host rock of the nickel mineralization grades from metapicrite to intrusive peridotite (Rantala metapicrite – Honkamäki hornblendite – Kiiskilänkangas peridotite).

Based on the whole rock Sm-Nd data (in total 58 samples analyzed for Sm-Nd isotopes) and chemistry of the Finnish Svecofennian mafic-ultramafic intrusions, metabasalts and metapicrites, Makkonen and Huhma (2008) concluded that the average composition of the metabasalts in the southern Savo area is equivalent to the proposed parental magma for the

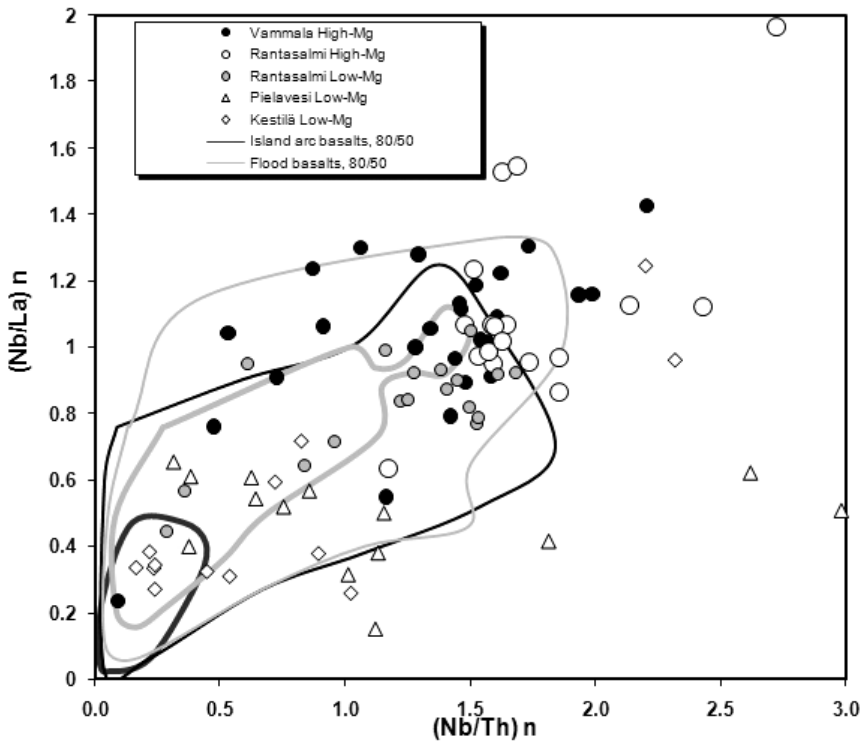


Fig. 7. Plot of primitive mantle-normalised Nb/La vs Nb/Th showing data from this paper compared with literature data from on-line Georoc database for island arc tholeiites (solid black outlines, 1187 samples) and continental flood basalts (solid grey outlines, 3777 samples). Density contours 50th and 80th percentiles.

Kotalahti Belt intrusions, composition of this magma being close to EMORB. The initial ϵ_{Nd} (1.9 Ga) values for the metapicrites are near +4 suggesting a depleted mantle source for the parental magma. The ϵ_{Nd} (1.9 Ga) values for the intrusions vary between +3.3 and -2.4 with the lowest values found in intrusions near the Archaean basement. Consequently, assimilation of upper crustal material was concluded to have lowered the ϵ_{Nd} values of intrusions. A simple bulk-mixing model between the proposed parental magma and Svecfennian metasediment/Archaean gneiss yielded initial ϵ_{Nd} values similar to those obtained from the intrusion samples. Assimilation of about 20 % by mass of Archaean gneiss is required to produce the lowest obtained initial ϵ_{Nd} value (-2.4) in intrusions.

Petrographically and geochemically similar metabasalts and metapicrites and of similar geological

setting to the metavolcanic rocks of this study occur widely around the Central Finland Granite Batholite (e.g. Gaál & Rauhamäki, 1971; Häkli et al., 1979; Kousa, 1985; Lahtinen, 1996, and references therein; Lehtonen et al., 2003; Makkonen, 1996; Peltonen, 1990; Schreurs et al., 1986). The age of these metavolcanic rocks has been estimated on geological basis to be c. 1.9 Ga. However, recently Väisänen & Kirkland (2008) published new U-Th-Pb zircon geochronology on igneous rocks in the Toijala and Salittu Formations, southwestern Finland. The Salittu Formation consists of EMORB-type tholeiitic basalts and picrites similar to the basalts and picrites of this study. Inner zircon domains in a felsic volcanic rock from the upper part of the Toijala Formation yielded an 1878 ± 4 Ma concordia age. This felsic rock includes also picritic rocks similar to the ones in the Salittu Formation, from which Väisänen & Kirkland

(2008) concluded that the age also applies to the lower part of the Salittu Formation. The age is the same as for most of the Svecofennian nickel-bearing intrusions in Finland (1.88 Ga, Peltonen, 2005). Thus, existing geological, geochemical and geochronological data support the comagmatism between the intrusions and metapicrites/tholeiites.

Geochemical data on mineralized and barren intrusions from the Kotalahti and Vammala Belts are shown in Fig. 6. The geochemical data on the intrusions in the Kotalahti Belt were collected during extensive nickel exploration projects by the Geological Survey of Finland in 1981–2001 (Makkonen, 1996; Forss et al., 1999; Makkonen et al., 2003). Data on the Vammala Belt intrusions are from Peltonen (1995c).

According to Makkonen et al. (2008), in the Kotalahti Belt the incompatible element concentrations are higher in mineralized intrusions than in barren ones. The most systematic difference is seen in Zr and P_2O_5 concentrations normalized to Ti. The REE contents are higher and the LREE are relatively more enriched in the mineralized lherzolites and harzburgites (Median Ce/Yb = 19.6) than in the barren ones (Median Ce/Yb = 9.6). The Ce/Yb and Th/Yb ratios are in all groups distinctly higher than in primitive mantle or NMORB. The highest values are found in mineralized intrusions.

Peltonen (1995b) concluded that the Vammala belt intrusions have trace element signatures comparable to those of modern arc tholeiites, while the picrites have signatures more akin to transitional MORBs, and on this basis the two suites are unrelated.

On the basis of the trace element patterns in the larger data set presented here, the evidence justifies a distinct petrogenetic origin for the intrusive and extrusive magmas in the Vammala area. The Vammala intrusion suite occupies a distinct field on the ratio-ratio plots with consistently low Ce/Sm and Zr/Yb and a range to lower Gd/Yb compared with most of the picrites. There is some degree of overlap with the more primitive members of the picrite suite, but in general the picrites appear less primitive than the intrusions on the basis of REE and Zr. However, the

opposite relationship is evident in Th contents, with the intrusions being notably higher in Th/Yb and Th/Nb compared with the picrites. This decoupling of Th from LREE is not explicable by contamination or alteration, so is likely to be inherited from the mantle source.

In the Kotalahti Belt in contrast, patterns for the intrusions are much more variable and dispersed than those for picrites (Fig. 5). This may be largely due to the fact that the intrusive rocks are cumulates and therefore have lower and more variable absolute levels, making them more susceptible to modification of low levels of trace elements by alteration (Barnes et al., 2004). Furthermore, they have almost certainly undergone local *in-situ* wall-rock contamination (Mäkinen & Makkonen, 2004; Makkonen & Huuhma, 2008). Broadly, the data set is consistent with a comagmatic origin for the Kotalahti Belt intrusions with the Rantasalmi low- and high-Mg suites, but with a substantial overprint of contamination and alteration, which largely obscures the original relationship.

The Vammala Belt intrusions, and to a lesser degree the Kotalahti Belt intrusions, are notably depleted in Ni for given MgO compared with picritic volcanic rocks (Fig. 4). This Ni depletion has been ascribed to *in situ* or flow conduit sulfide segregation (Peltonen, 1995a; Makkonen, 1996; Mäkinen & Makkonen, 2004; Makkonen et al., 2008). *In situ* sulfide segregation implies that the lavas cannot be interpreted as magma which has flowed through the intrusions leaving behind sulfide mineralisation. While the lavas and the intrusions may well ultimately be comagmatic, the magmas appear to have followed different plumbing systems through the crust, such that the signatures of mineralization and contamination are much more evident in the intrusions.

5. PGE Variations and Sulfur Saturation

Variations of PGE contents in low-sulfur rocks are very sensitive indicators of the presence or absence of sulfide liquid saturation (referred to here as sulfur sat-

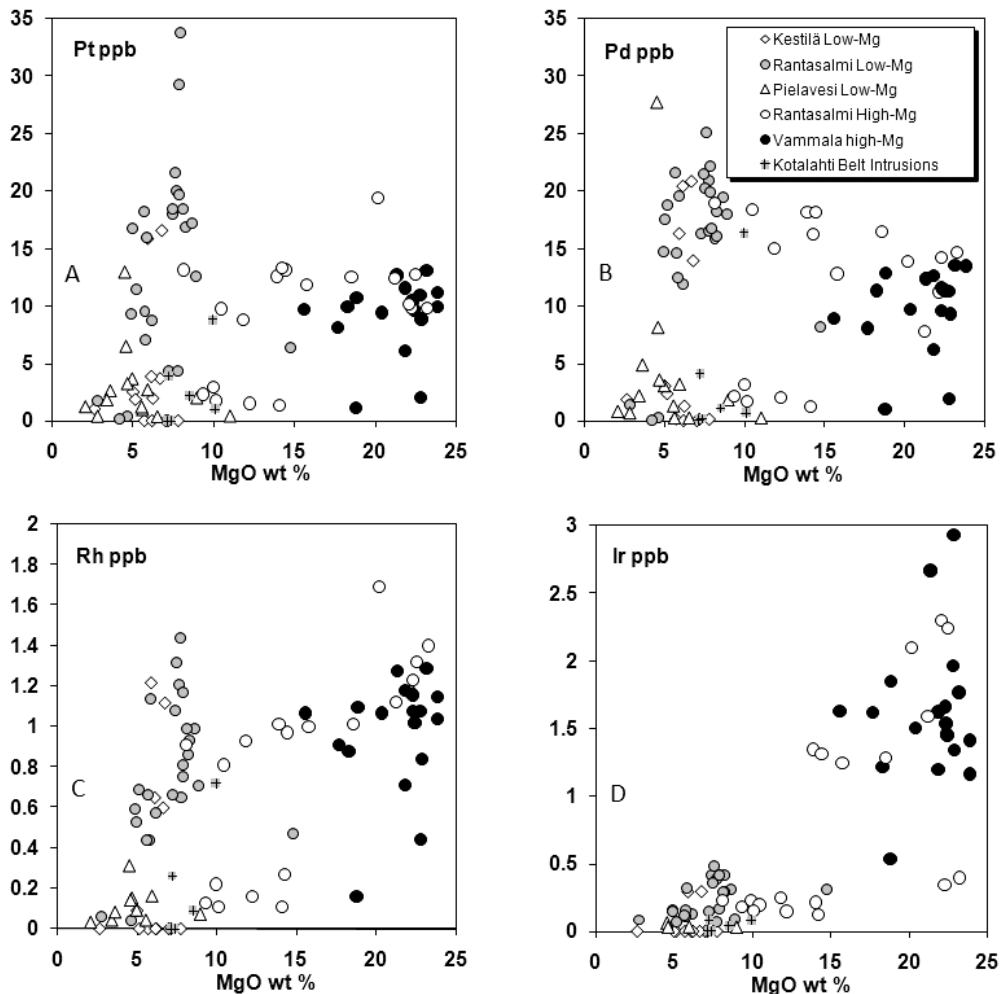


Fig. 8. Plots of PGE vs MgO in S-poor samples. Data recalculated to 100% volatile-free.

uration) during evolution of a magma series, owing to the extremely high partition coefficients of PGEs into sulfides (Fleet et al., 1991). The PGE (Pt, Pd, Ir, Ru and Rh) in the present study define distinctly different behavior between high-Mg and low-Mg suites (both Rantasalmi and Pielavesi) when plotted against MgO content (Fig. 8).

In the Rantasalmi high-Mg suite, Pt and Pd show approximately constant or slightly increasing abundances with declining MgO, that is in rocks with lower abundances of olivine, while Ir and Rh behave as compatible elements, declining with decreasing MgO (decreasing olivine content). In the case of Ir and Rh,

this type of trend has been explained by partitioning of these elements into olivine and co-crystallizing chromite (Brenan et al., 2005; Sattari et al., 2002), as commonly observed in komatiites and other olivine-saturated magmas (Barnes et al., 1985; Puchtel & Humayun, 2001; Puchtel et al., 2004). Based on detailed analysis of IPGE trends in komatiites, Barnes and Fiorentini (2008) favor control by IPGE-rich magmatic phases such as laurite or Ir-Os alloy co-crystallizing with olivine.

Sulfide-controlled fractionation behavior of Pt and Pd in the high-Mg rocks is more evident when the elements are shown as ratios against Ti, to take out

the effect of fractionation and accumulation of olivine, plagioclase or pyroxene (Fig. 9). Ratios are shown normalized against estimated mantle abundances from Barnes et al. (1988). The plot of normalized Pt/Ti vs MgO also shows the results of numerical modeling of fractional and equilibrium crystallization of an idealized Rantasalmi picrite composition, assuming a starting liquid with 15 % MgO and 15 ppb Pt. Major element compositions were calculated using the MELTS program (Ghiorso & Sack, 1995), and Pt behavior was calculated assuming a bulk partition coefficient into the sulfide-liquid bearing crystallizing assemblage and using the standard Shaw equations. The model curves show that even very small amounts of fractional segregation of sulfide liquid are capable of dramatically lowering the Pt/Ti and Pd/Ti ratios of the residual silicate liquid. The abundance of sulfide in the fractionating assemblage is described by the parameter R_x , defined as the mass ratio of silicate to sulfide liquid being extracted; steep declines with MgO are predicted for values of R_x as high as 500, owing to the extremely high value (taken as 10,000) of the partition coefficient D_{Pt} between sulfide and silicate melt. An R_x of 500 corresponds to 0.2 wt.% sulfide liquid in the fractionating assemblage. In nature, the effective value of the bulk D (given by the ratio D_{Pt}/R_x) may be lower than the true thermodynamic value for kinetic reasons (Mungall, 2002), perhaps by an order of magnitude or more, but the extent of PGE depletion would still be very high for sulfide proportions in the fractionating assemblage of the order of a percent.

Within the Rantasalmi high-Mg suite, Pt/Ti is constant or slightly decreasing with decreasing MgO, while Pd/Ti remains roughly constant, except for the lowest-Mg samples. The data imply that the most olivine-rich samples were erupted sulfur-undersaturated, and the trend in the samples above about 10 % MgO is due to accumulation of olivine in the absence of sulfide. The low Pt/Ti and Pd/Ti ratios in a group of five lower-Mg samples (all from the Pirilä locality) implies that sulfur saturation was attained in these lower Mg rocks, probably as a result of olivine fractionation within the suite. With this exception,

the Rantasalmi high-Mg suite was emplaced sulfur-undersaturated.

With the exception of a group of Pt- and Pd-depleted samples, all from the Stormi area, the same conclusion applies to the Vammala high-Mg volcanic suite, which is closely similar in PGE contents to the Rantasalmi high-MgO rocks. However, these anomalous samples, which also include one sample each from the Ruotsila and Komerolahti areas, imply that a component of S-saturated magma is present within the suite.

Samples from the Rantasalmi low-Mg suite define a steep trend of widely variable Pt/Ti and Pd/Ti, roughly parallel to the model trend predicted for sulfide liquid fractionation. The Pd vs. MgO plot shows that the low-Mg suite rocks fall on the low-Mg end of the trend defined by the Rantasalmi high-Mg suite, consistent with their being part of the same suite of sulfur-undersaturated magmas. The Rantasalmi low-Mg suite was erupted for the most part sulfur-undersaturated, but some of the more evolved members attained sulfur saturation with fractionation.

In contrast, and with the exception of a few overlapping samples, the Pielavesi and Kestilä low-Mg suites appear to have been pervasively sulfur saturated, having markedly depleted PGEs and low PGE:Ti ratios in most samples. These ratios are consistently lower than the commonly assumed mantle value (or less than 1 on the mantle normalized plot). This implies that mantle source regions were sub-chondritic with respect to PPGE (Pt, Pd and Rh).

The data imply a simple geographical separation within the Kotalahti Nickel Belt: lavas in the south-east of the belt, from the Rantasalmi, Savonlinna and Juva areas, were erupted predominantly sulfur undersaturated, while those further to the north-west were predominantly sulfur saturated. The PGE data are consistent with the conclusion that the Rantasalmi low- and high-MgO suites are in fact part of a single coherent grouping. Variable degrees of crustal contamination within the suites did not induce sulfur saturation, except locally in the more evolved rocks.

There is no significant relationship between Pt/Pd ratio and MgO through the entire data set, with

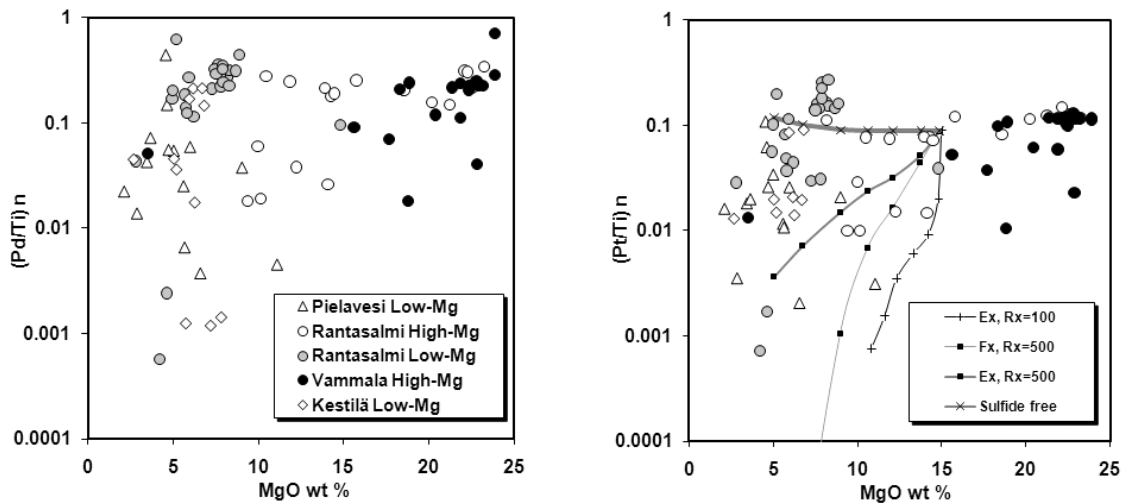


Fig. 9. Plots of primitive mantle-normalised PGE/Ti ratio vs MgO. Normalising values from Barnes et al. (1988). Model curves represent numerical simulation of fractional crystallization (Fx) and batch equilibrium crystallization (Ex) of an idealised average picrite liquid, with a starting composition of MgO 15 % and 15 ppb Pt. Major element modelling with the MELTS program (Ghiorso & Sack, 1995) and Pt modelling with the standard Shaw equations. The abundance of sulfide in the fractionating assemblage is described by the parameter R_x , defined as the mass ratio of silicate to sulfide liquid being extracted; the partition coefficient D_{Pt} between sulfide and silicate melt is taken as 10 000 based on references cited in the text. Ticks on curves are in temperature increments of 20 °C.

mantle-normalized ratios varying unsystematically between about 0.3 and 0.8 with occasional outliers (Fig. 9). This implies that these elements were not fractionated from one other, consistent with sulfide liquid control and similar partition coefficients.

Two samples from the RLM suite (Harjula and Kukonkivi) show anomalously high Pt values, but are typical of the suite in all other respects. The relationship between these samples and others is further explored in Figure 10, which shows the inter-element relationships between the PPGE (Pt, Pd and Rh) and IPGE (Ir and Ru) for all the volcanic samples. A number of distinctive features emerge from these plots.

1. There is a strong positive correlation within all the suites between Pt and Pd, and to a lesser degree between Pt and Rh (Figs. 10a and f). The positive correlation between Pt, Pd and Rh in the VHM, RHM and RLM suites is interpreted as the result of variable enrichment of these elements during silicate fractionation in the absence of sulfur saturation.

2. The Pt-rich samples from the RHM suite are anomalous in falling well below the correlation line for both Pd and Rh (Figs. 10a and f); the enrichment in Pt is double that for the other PPGE. These samples fall at the top of the range of RLM samples for Pt/Ti, having about doubled the average value (Table 5). The likely explanation, consistent with the generally higher degree of scatter in the RLM suite, is that there has been a minor degree of mobilization of the PPGE during alteration, and these anomalous samples have had their Pt contents boosted.
3. PPGE and IPGE are completely decoupled, but correlations between the IPGE (Ir and Ru) are strong. This clearly reflects distinct geochemical controls; Ir and Ru both behave as compatible elements, and are significantly depleted in the high-Mg relative to the low-Mg suites. The generally strong correlation between Ir, Ru and Rh in the high-Mg suites implies control by a common phase, probably an alloy phase on the liquidus during fractionation and accumulation

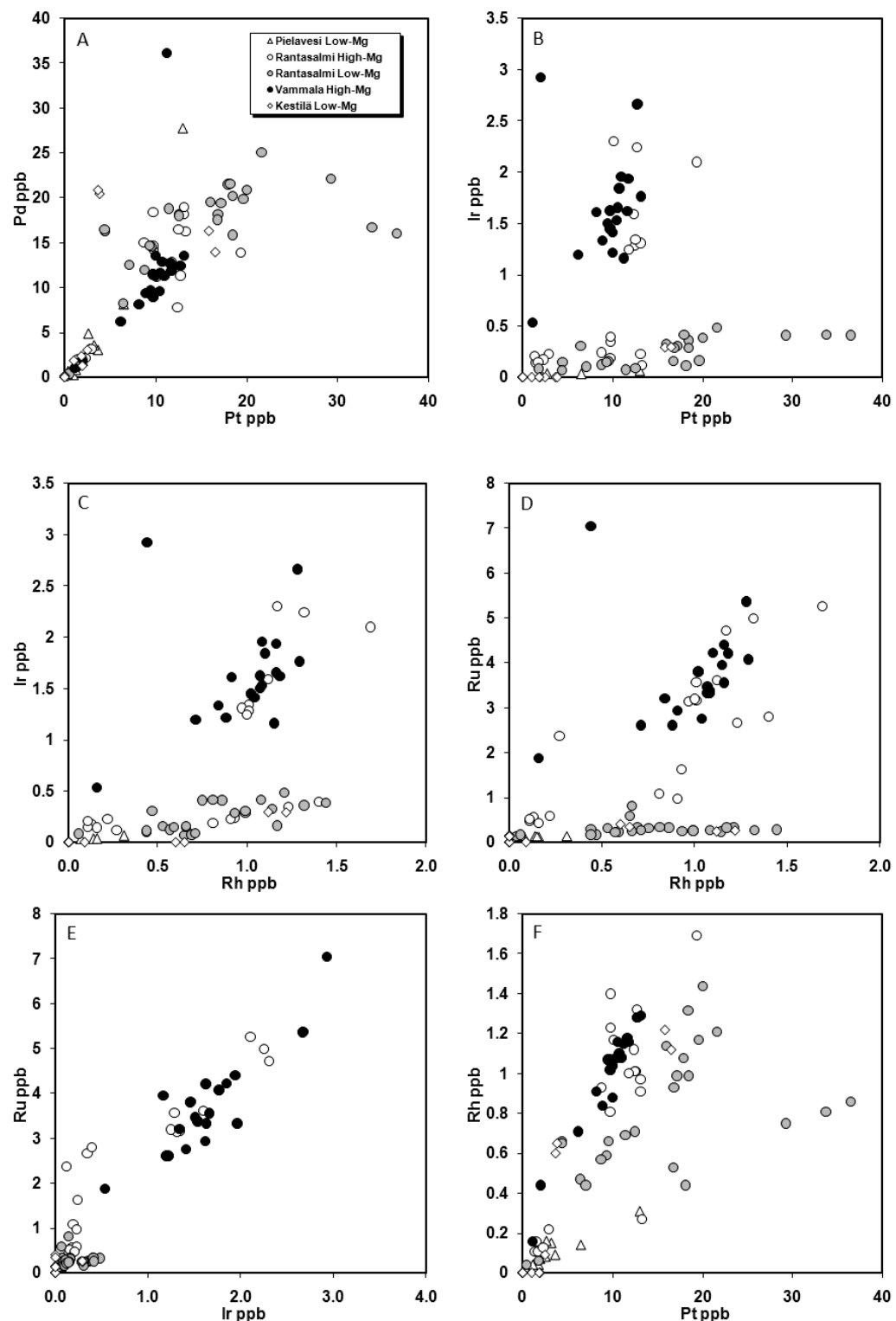


Fig. 10. Plot of inter-element variations among PGE, for the volcanic suites only. Data recalculated to 100 % volatile-free.

of olivine (Barnes & Fiorentini, 2009). A single Vammala High-Mg suite sample, from the mineralized Stormi area, contains anomalously high Ir and Ru, without correspondingly high Rh. This sample falls on the Ir-Ru correlation trend. A possible explanation is that this sample contains accumulated grains of magmatic Ir-Ru alloy.

4. The RHM and VHM suites show close similarity according to most of the geochemical criteria we have considered, including the PGE trends, consistent with a comagmatic origin, and consistent with sulfur-undersaturated character for all but a small number of relatively Mg-poor samples.
5. The RLM suite shows a distinctly different Pt/Rh ratio from that of the RHM suite. The slightly lower Rh content for the same Pt implies a mild degree of compatibility for Rh, such that it is slightly depleted relative to Pt in the more evolved liquids (Fig. 10f).

6. Conclusions

The amphibolite-picrite samples from the Kotalahti and Vammala Belts can be divided into five suites with distinctive chemical characteristics.

Rantasalmi High-Mg Suite and Vammala High-Mg suites include tholeiites and tholeiitic picrites with a range of olivine contents, related by fractional crystallization and accumulation of olivine and chromite. These lavas were for the most part erupted sulfur-undersaturated. PGE depletion due to sulfide liquid fractionation is evident in a small number of fractionated Rantasalmi samples, and in Vammala samples from the Stormi area. Trace element data indicate a component of crustal contamination, with a metasomatic overprint due to variable degrees of pre- and/or syn-metamorphic alteration. Parental magmas were relatively primitive and had near-chondritic immobile trace element signatures, consistent with a plume origin.

Rantasalmi Low-Mg Suite is characterized by fractionated tholeiite compositions with little or no crust-

al contamination, strongly clustered major element compositions implying control by low-pressure fractionation and multiple phase saturation, sulfur-undersaturated, and locally metasomatised during potassic alteration. These are probably comagmatic with the high-Mg suite. A trend of silica enrichment with decreasing MgO cannot be explained by fractional crystallization and is probably a consequence of silicification during alteration.

Kestilä low-Mg suite is similar to the Rantasalmi low-Mg suite, but distinguished from it by clear evidence for pre-eruption sulfur saturation.

Pielavesi low-Mg suite is composed of fractionated island arc tholeiites, heavily modified by metasomatic alteration, predominantly sulfur-saturated, and probably unrelated to the Rantasalmi and Kestilä low-Mg suite.

On the basis of major and trace element chemistry, the conclusion of Peltonen (1995b) that the Vammala picrites are unrelated to the intrusions is permissive, but cannot be conclusively proven. There is considerable overlap in incompatible trace element signatures, taking into account the more extensive effects of contamination (and possibly alteration) in the intrusions. Nickel–MgO element trends are not colinear between picrite and intrusions, implying that the picrites cannot simply be related to the intrusions by entrainment of olivine. There has been some divergent evolution, probably through low-pressure fractionation. The intrusions have undergone an episode of nickel depletion, presumably due to sulfide extraction, not seen in the picrites. It is likely that the intrusion parent magmas and picrite magmas had a common mantle source but have evolved along distinct paths, and the picrites probably do not represent parent magmas tapped directly from the intrusions.

The Vammala Belt picrites are remarkably similar to the more Mg-rich end of the Rantasalmi picrite suite in the Kotalahti Belt, supporting a comagmatic origin. They fall into two groups in their PGE contents, an undepleted group, like the Rantasalmi picrites, which were evidently erupted sulfur-undersaturated, and depleted group mainly found in the Stormi area.

The PGE data in the Kotalahti Belt metavolcanic rocks imply a simple geographical separation. As a generalization, lavas in the south-east of the belt, that is from the Rantasalmi, Savonlinna and Juva areas were erupted sulfur-undersaturated, while those further to the North West were sulfur-saturated. These spatial differences suggest that the PGE contents of the metavolcanic rocks can be used as regional area selection criteria for intrusive nickel-copper-(PGE) deposits within the Finnish Svecfennian.

On the basis of available data it is however, difficult to conclude whether the PGE depletion in metavolcanic rocks is always present in association with mineralized intrusions. In Stormi area the association is clear, but in the in Rantasalmi, Savonlinna and Juva sampling areas, located at 10–15 km distance from to the intrusive nickel deposits, PGE depletion is absent. Magma evidently took different routes into the upper crust to produce the intrusive and extrusive phases. Sulfur saturation can be achieved in an intrusion *in situ* or close to the present intrusive body. An earlier eruptive phase of the same magma can thus be sulfur-undersaturated, as illustrated in Figure 2, such that the absence of a PGE depleted signal gives a false negative indication of mineralization potential. PGE depletion at ten-kilometre scale appears to be a sensitive indicator of the regional nickel sulfide potential, but finer-scale targeting than this appears to be unsupported by the data.

Acknowledgments

This study is based on the results of a collaborative research project involving CSIRO and the Geological Survey of Finland (GTK). The authors extend their appreciation to both of these organizations and to TEKES (National Technology Agency of Finland) for their financial support for the project. Dr. Eero Hanski and Dr. Wolf Maier as the reviewers of this publication are acknowledged for their constructive comments. Jukka Kousa (GTK) helped us to select the samples in the NW part of the Kotalahti Nickel Belt. Michael Hart of CSIRO performed the XRF analyses. PGE and ICP-MS analyses were performed

at Geoscience Laboratories in Sudbury, and we thank Merilla Clement and the staff of the laboratory for their painstaking work. We thank Dr. Mark Ghiorso for assistance with the MELTS modelling software. Dr. Brent McInnes and Dr. Peter Momme provided some helpful comments on the first draft of the manuscript.

References

- Barnes, S.-J., Boyd, R., Nilsson, L., Often, M., Pedersen, R.B. & Robins, B., 1988. The use of mantle normalization and metal ratios in discriminating between the effects of partial melting, crystal fractionation and sulfide segregation on platinum group metals, gold, nickel and copper: examples from Norway. In: Prichard, H.M., Potts, P.J., Bowles, J.F.W. & Cribb, S.J. (eds.) *Geo-Platinum 87*. Elsevier, pp. 113–139.
- Barnes, S.-J., Naldrett, A.J. & Gorton, M.P., 1985. The origin of the fractionation of the platinum-group elements in terrestrial magmas. *Chemical Geology* 53, 303–323.
- Barnes, S.-J., Couture, J.-F., Sawyer, E.W. & Bouchaib, C., 1993. Nickel-copper occurrences in the Belleterre-Angliers Belt of the Pontiac Subprovince and the use of Cu/Pd ratios in interpreting platinum-group element distributions. *Economic Geology* 88, 1402–1418.
- Barnes, S.-J., Melezhik, V.A. & Sokolov, S.V., 2001. The composition and mode of formation of the Pechenga nickel deposits, Kola Peninsula, northwestern Russia. *Canadian Mineralogist* 39, 447–471.
- Barnes, S.-J. & Picard, C.P., 1993. The behavior of platinum-group elements during partial melting, crystal fractionation, and sulphide segregation: an example from the Cape Smith Fold Belt, Northern Quebec. *Geochimica et Cosmochimica Acta* 57, 79–87.
- Barnes, S.J. & Fiorentini, M.L., 2008. Iridium, ruthenium and rhodium in komatiites: evidence for iridium alloy saturation. *Chemical Geology* 257, 44–58.
- Barnes, S.J., Hill, R.E.T., Perring, C.S. & Dowling, S.E., 2004. Lithogeochemical exploration for komatiite-associated Ni-sulfide deposits: strategies and limitations. *Mineralogy and Petrology* 82, 259–293.
- Boyd, R., Barnes, S.-J. & Gronlie, A., 1988. Noble metal geochemistry of some Ni-Cu deposits in the Sveconorwegian and Caledonian orogens in Norway. In: Prichard, H.M., Potts, P.J., Bowles, J.F.W. & Cribb, S.J. (eds.) *Geo-Platinum 87*. Elsevier, pp. 22–43.
- Boyd, R. & Mathieson, C.O., 1979. The nickel mineralisation of the Råna mafic intrusion, Nordland, Norway. *Canadian Mineralogist* 17, 287–298.
- Brenan, J.M., McDonough, W.F. & Ash, R., 2005. An experimental study of the solubility and partitioning of iridium, osmium and gold between olivine and silicate melt. *Earth and Planetary Science Letters* 237, 855–872.

- Brügmann, G.E., Naldrett, A.J., Asif, M., Lightfoot, P.C., Gorbachev, N.S. & Fedorenko, A., 1993. Siderophile and chalcophile metals as tracers of the evolution of the Siberian Trap in the Noril'sk region, Russia. *Geochimica et Cosmochimica Acta* 57, 2001–2018.
- Ekdahl, E., 1993. Early Proterozoic Karelian and Svecofennian formations and the evolution of the Raahē–Ladoga Ore Zone, based on the Pielavesi area, central Finland. Geological Survey of Finland, Bulletin 373, 1–137.
- Fleet, M.E., Crocket, J.H., Liu, M.H. & Stone, W.E., 1999. Laboratory partitioning of platinum-group elements (PGE) and gold with application to magmatic sulfide–PGE deposits. *Lithos* 47, 127–142.
- Fleet, M.E., Stone, W.E. & Crocket, J.H., 1991. Partitioning of palladium, iridium and platinum between sulfide liquid and basalt melt: effects of melt composition, concentration and oxygen fugacity. *Geochimica et Cosmochimica Acta* 55, 2545–2554.
- Forss, H., Kontoniemi, O., Lempäinen, R., Luukas, J., Makkonen, H. & Mäkinen, J., 1999. Ni-vyöhyke ja 1. 9 Ga magmatismi-hankkeen (12204) toiminta vuosina 1992–1998 Tervo–Varkaus-alueella. Geological Survey of Finland, Archive report, M 19/3241/99/1/10. 152 pp. (In Finnish with English abstract and figure/table captions)
- Gaál, G., 1972. Tectonic control of some Ni-Cu deposits in Finland. In: Gill, J.E., (ed.) International Geological Congress, 24th session, Montreal 1972. Section 4, Mineral deposits, 215–224.
- Gaál, G. & Rauhamäki, E., 1971. Petrological and structural analysis of the Haukivesi area between Varkaus and Savonlinna, Finland. *Bulletin of the Geological Society of Finland* 43, 265–337.
- Gaál, G., 1980. Geological setting and intrusion tectonics of the Kotalahti nickel-copper deposit, Finland. *Bulletin of the Geological Society of Finland* 52, 101–128.
- Ghiorso, M.S. & Sack, R.O., 1995. Chemical mass-transfer in magmatic processes. 4. a revised and internally consistent thermodynamic model for the interpolation and extrapolation of liquid-solid equilibria in magmatic systems at elevated temperatures and pressures. *Contributions to Mineralogy and Petrology* 119, 197–212.
- Grundström, L., 1980. The Laukunkangas nickel-copper occurrence in southeastern Finland. *Bulletin of the Geological Society of Finland* 52, 23–53.
- Häkli, T.A., Vormisto, K. & Hänninen, E., 1979. Vammala, a nickel deposit in layered ultramafite, Southwest Finland. *Economic Geology* 74, 1166–1182.
- Hill, R., Barnes, S.J., Dowling, S., Makkonen, H. & Peltonen, P. 2005. Chalcophile element distribution in mafic and ultramafic metavolcanic rocks of the Svecofennian Kotalahti and Vammala nickel belts Finland – a test for a geochemical signature of subvolcanic magmatic ore forming processes. Regional area selection criteria for intrusive Ni/Cu sulfide ore deposits. Final Report. CSIRO, GTK. Geological Survey of Finland, Archive report, M 10.4/2005/2.
- Hölttä, P., 1988. Metamorphic zones and the evolution of granulite grade metamorphism in the early Proterozoic Pielavesi area, central Finland. Geological Survey of Finland, Bulletin 344, 1–50.
- Hulbert, L.J., Hamilton, M.A., Horan, M.F. & Scoates, R.F.J., 2005. U-Pb Zircon and Re-Os isotope geochronology of mineralized ultramafic intrusions and associated nickel ores from the Thompson Nickel Belt, Manitoba, Canada. *Economic Geology* 100, 29–41.
- Kilpeläinen, T., 1998. Evolution and 3D modelling of structural and metamorphic patterns of the Palaeoproterozoic crust in the Tampere–Vammala area, southern Finland. Geological Survey of Finland, Bulletin 397, 1–124.
- Koistinen, T.J., 1981. Structural evolution of an early Proterozoic stratabound Cu-Co-Zn deposit, Outokumpu, Finland. *Transactions of the Royal Society of Edinburgh: Earth Sciences* 72, 115–158.
- Koistinen, T., Klein, V., Koppelmaa, H., Korsman, K., Lahtinen, R., Nironen, M., Puura, V., Saltykova, T., Tikhomirov, S. & Yanovskiy, A., 1996. Paleoproterozoic Svecofennian orogenic belt in the surroundings of the Gulf of Finland. In: Koistinen, T.J., (ed.) Explanation to the map of Precambrian basement of the Gulf of Finland and surrounding area 1 : 1 mill. Geological Survey of Finland, Special Paper 21, 21–57.
- Korsman, K., Hölttä, P., Hautala, T. & Wasenius, P. 1984. Metamorphism as an indicator of evolution and structure of the crust in Eastern Finland. Geological Survey of Finland, Bulletin 328, 1–40.
- Korsman, K., Koistinen, T., Kohonen, J., Wennerström, M., Ekdahl, E., Honkamo, M., Idman, H. & Pekkala, Y., (eds.) 1997. Suomen kallioperäkartta = Berggrundskarta över Finland = Bedrock map of Finland 1:1 000 000. Espoo, Geological Survey of Finland.
- Kousa, J., 1985. Rantasalmen tholeiitisista ja komatiittisista vulkaniiteista. Summary: The tholeiitic and komatiitic metavolcanic rocks in Rantasalmi, Southeastern Finland. *Geologi* 37, 17–22.
- Kousa, J. & Lundqvist, T., 2000. Meso- and Neoproterozoic cover rocks of the Svecofennian Domain. In: Lundqvist, T. & Autio, S., (eds.) Description to the bedrock map of central Fennoscandia (Mid-Norden). Geological Survey of Finland, Special Paper 28, 75–76.
- Lahtinen, R. 1996. Geochemistry of Palaeoproterozoic supracrustal and plutonic rocks in the Tampere–Hämeenlinna area, southern Finland. Geological Survey of Finland, Bulletin 389, 1–113.
- Lamberg, P., 2005. From genetic concepts to practice – litho-geochemical identification of Ni-Cu mineralized intrusions and localisation of the ore. Geological Survey of Finland, Bulletin 402, 1–264.
- Lehtonen, M.I., Kujala, H., Kärkkäinen, N., Lehtonen, A., Mäkitie, H., Määntäri, I., Virransalo, P. & Vuokko, J., 2005. Etelä-Pohjanmaan liuskealueen kallioperä. Sum-

- mary: Pre-Quaternary rocks of the South Ostrobothnian Schist Belt. Geological Survey of Finland, Report of Investigation 158, 1–155.
- Mäkinen, J., 1987. Geochemical characteristics of Svecokarelicid mafic-ultramafic intrusions associated with Ni-Cu occurrences in Finland. Geological Survey of Finland, Bulletin 342, 1–109.
- Mäkinen, J. & Makkonen, H.V., 2004. Petrology and structure of the Palaeoproterozoic (1.9 Ga) Rytty nickel sulfide deposit, Central Finland: a comparison with the Kotalahti nickel deposit. *Mineralium Deposita* 39, 405–421.
- Makkonen, H.V., 1996. 1.9 Ga tholeiitic magmatism and related Ni-Cu deposition in the Juva area, SE Finland. Geological Survey of Finland, Bulletin 386, 1–101.
- Makkonen, H.V., 2005. Intrusion model for Svecofennian (1.9 Ga) mafic-ultramafic intrusions in Finland. In: Autio, S., (ed.) Current Research 2003–2004. Geological Survey of Finland, Special Paper 38, 11–14.
- Makkonen, H., Kontoniemi, O., Lempäinen, R., Lestinen, P., Mursu, J. & Mäkinen, J., 2003. Raahe–Laatokka-vyöhyke, nikkelin ja kullan etsintä-hankkeen (2108001) toiminta vuosina 1999–2003. Geological Survey of Finland, Archive report, M 10.4/2003/5/10. 90 pp. (In Finnish with English abstract and figure/table captions)
- Makkonen, H.V., Mäkinen, J. & Kontoniemi, O., 2008. Geochemical discrimination between barren and mineralized intrusions in the Svecofennian (1.9 Ga) Kotalahti Nickel Belt, Finland. *Ore Geology Reviews* 33, 101–114.
- Marshall, B., Smith, J.V. & Mancini, F., 1995. Emplacement and implications of peridotite-hosted leucocratic dykes, Vammala Mine, Finland. *GFF* 117, 199–205.
- McDonough, W.F. & Sun, S.-s., 1995. The composition of the Earth. *Chemical Geology* 120, 223–253.
- Meisel, T., Moser, J., Fellner, N., Wegscheider, W. & Schoenberg, R., 2001. Simplified method for the determination of Ru, Pd, Re, Os, Ir, and Pt in chromitites and other geological materials by isotope dilution ICP-MS and acid digestion. *Analyst* 126, 322–328.
- Mungall, J.E., 2002. Kinetic controls on the partitioning of trace elements between silicate and sulfide liquids. *Journal of Petrology* 43, 749–768.
- Papunen, H. & Gorbunov, G.I., (eds.) 1985. Nickel–copper deposits of the Baltic Shield and Scandinavian Caledonides. Geological Survey of Finland, Bulletin 333, 1–394.
- Peach, C.L. & Mathez, E.A., 1996. Constraints on the formation of platinum-group element deposits in igneous rocks. *Economic Geology* 91, 439–450.
- Pekkarinen, L.J., 2002. Haukivuoren ja Pieksämäen karttalualueiden kallioperä. Summary: Pre-Quaternary rocks of the Haukivuori and Pieksämäki map-sheet areas. Suomen geologinen kartta 1:100 000: kallioperäkarttojen selitykset lehdet 3231+3232. Geological Survey of Finland. 98 pp.
- Peltonen, P. 1990. Metamorphic olivine in picritic metavolcanics from southern Finland. *Bulletin of the Geological Society of Finland* 62, 99–114.
- Peltonen, P., 1995a. Magma-country rock interaction and the genesis of Ni-Cu deposits in the Vammala Nickel Belt, SW Finland. *Mineralogy and Petrology* 52, 1–24.
- Peltonen, P., 1995b. Petrogenesis of ultramafic rocks in the Vammala Nickel Belt: implications for crustal evolution of the early Proterozoic Svecofennian arc terrane. *Lithos* 34, 253–274.
- Peltonen, P., 1995c. Whole-rock analyses of ultramafic rocks, Vammala Ni-belt, southwestern Finland. Geological Survey of Finland, Archive report, K/31.82/2121/94/1. 6 pp.
- Peltonen, P., 2005. Svecofennian mafic-ultramafic intrusions. In: Lehtinen, M., Nurmi, P.A. & Rämö, O.T., (eds.). *Precambrian Geology of Finland – key to the evolution of the Fennoscandian Shield. Developments in Precambrian Geology* 14, 407–442.
- Philipp, H., Eckhardt, J.D. & Puchelt, H., 2001. Platinum-group elements (PGE) in basalts of the seaward-dipping reflector sequence, SE Greenland coast. *Journal of Petrology* 42, 407–432.
- Plessen H.G. & Erzinger J., 1988. Determination of the platinum-group elements and gold in twenty rock reference materials by inductively coupled plasma mass spectrometry (ICP-MS) after preconcentration by nickel sulfide fire assay. *Geostandards Newsletter* 22, 187–194.
- Puchtel, I.S. & Humayun, M., 2001. Platinum group element fractionation in a komatiitic basalt lava lake. *Geochimica et Cosmochimica Acta* 65, 2979–2993.
- Puchtel, I.S., Humayun, M., Campbell, A.J., Sproule, R.A. & Lesher, C.M., 2004. Platinum group element geochemistry of komatiites from the Alexo and Pyke Hill areas, Ontario, Canada. *Geochimica et Cosmochimica Acta* 68, 1361–1383.
- Puustinen, K., Saltikoff, B. & Tontti, M. 1995. Distribution and metallogenic types of nickel deposits in Finland. Geological Survey of Finland, Report of Investigation 132, 1–38.
- Rouhunkoski, P., 1968. On the geology and geochemistry of the Vihanti zinc ore deposit, Finland. *Bulletin de la Commission géologique de Finlande* 236, 1–121.
- Sattari, P., Brenan, J.M., Horn, I. & McDonough, W.F., 2002. Experimental constraints on the sulfide- and chromite-silicate melt partitioning behavior of rhenium and platinum-group elements. *Economic Geology* and the *Bulletin of the Society of Economic Geologists* 97, 385–398.
- Schreurs, J., Kooperen, P. van & Westra, L. 1986. Ultramafic metavolcanic rocks of early proterozoic age in West-Uusimaa, SW Finland. *Neues Jahrbuch für Mineralogie, Abhandlungen* 155, 185–201.
- Song, X., Zhou, M., Keays, R., Cao, Z., Sun, M. & Qi, L., 2006. Geochemistry of the Emeishan flood basalts at Yangliuping, Sichuan, SW China: implications for

- sulfide segregation. *Contributions to Mineralogy and Petrology* 152, 53–74.
- St. Onge, M.R., Lucas, S.B. & Scott, D.J., 1997. The Ungava Orogen and the Cape Smith Thrust Belt. In: De Wit, M.J. & Ashwal, L.D., (eds.) *Greenstone Belts*. Oxford University Press, pp. 772–780.
- Tuisku, P. & Makkonen, H.V., 1999. Spinel-bearing symplectites in Palaeoproterozoic ultramafic rocks from two different geological settings in Finland: thermobarometric and tectonic implications. *GFF* 121, 293–300.
- Vaasjoki, M. & Sakkö, M., 1988. The evolution of the Raahe–Ladoga zone in Finland: isotopic constraints. In: Korsman, K., (ed.) *Tectono-metamorphic evolution of the Raahe-Ladoga zone*. Geological Survey of Finland, Bulletin 343, 7–32.
- Vaasjoki, M. & Kontoniemi, O., 1991. Isotopic studies from the Proterozoic Osikomäki gold prospect at Rantasalmi, southeastern Finland. In: Autio, S., (ed.) *Current Research 1989–1990*. Geological Survey of Finland, Special Paper 12, 53–57.
- Väistönen, M. & Kirkland, C.L. 2008. U-Th-Pb zircon geochronology on igneous rocks in the Toijala and Salittu Formations, Orijärvi area, southwestern Finland: constraints on the age of volcanism and metamorphism. *Bulletin of the Geological Society of Finland* 80, 73–87.
- Zhang, X., 2000. Geochemical exploration for polymetallic ores in volcano-sedimentary rocks: studies in China and Finland. *Acta Universitatis Ouluensis, Series A, Scientiae Rerum Naturalium* 352, 1–140.